LEVEL II

DILATANCY INSTABILITY AS A POSSIBLE SEISMIC MECHANISM

Contract No. 14-08-0001-12859
ARPA Order No. 1684

James E. Russell

Department of Mining Engineering
South Dakota School of Mines & Technology
Rapid City, South Dakota 57701

(1)

FINAL REPORT

Title: Dilatancy Instability as a Possible Seismic Mechanism

Principal Investigator: James E. Russell
Professor of Mining Engineering
South Dakota School of Mines & Technology
Rapid City, South Dakota 57701

Contract Period: April 10, 1972 to November 30, 1973

Sponsored by: The U. S. Geological Survey
Contract No. 14-08-0001-12859
Under ARPA Order No. 1684

Government Technical Officer: Dr. C. B. Raleigh
Program Manager

Final Report Submitted: June 1976

Disclaimer: The views and conclusions contained in this document are those of the author and should not be interpreted as necessarily representing the official policies, either expressed or implied, of the U. S. Government.

ABSTRACT

Dilatancy instability as a possible seismic mechanism is studied theoretically, numerically, and experimentally in the laboratory. The theoretical study concentrates on the fundamental nature of mechanical instability.

The numerical portion of the study consists of the development of a 1-dimensional model that couples fluid flow phenomena with a sliding block model. Fluid injection and withdrawal experiments can be run on the numerical model to verify the results of the theoretical study.

The experimental phase of the study concentrated on measuring dilatancy behavior of intact samples of Weber Sandstone under triaxial conditions using both a hydraulic system and electrical resistance strain gages. Results indicate that the volumetric behavior of the sandstone samples tested is similar to that reported by other investigators for dense sand.

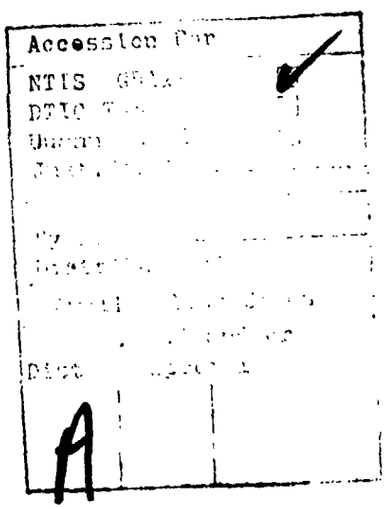

TABLE OF CONTENTS

LIST OF TABLES AND FIGURES

1. GENERAL INTRODUCTION

1.1 Dilatancy and its Relation to Discontinuum and Continuum Behavior

The term dilatancy was originally defined by Osborne Reynolds (1885) who referred to dilatancy as a property of granular media. Reynolds states, "I have called this unique property 'dilatancy', because the property consists in a definite change of bulk, consequent on a definite change of shape or distortional strain, any disturbance whatever causing a change of volume and generally dilation." Frank (1966) defines the term consistently but more concisely as "the property possessed by granular masses of expanding in bulk with change in shape." The concept of a relationship between bulk behavior (changes in volume) and distortional behavior (changes in shape) is foreign to linear continuum theories where bulk behavior is assumed to be independent of distortional behavior. Considering dilatancy in terms of the conservation of mass, it is obvious that the change in volume of a granular mass that accompanies a change in shape is possible only by rearrangement of the constituent grains. This rearrangement of grains alters the pore volume and hence the porosity of the mass. In a granular medium, an increase in porosity generally leads to an increase in permeability.

Dilatancy is a commonly observed phenomena in soil mechanics and much literature is available on the topic, particularly on sand, for example, Finn et. al. (1967), Lee and Seed (1967), Vesic and Clough (1968), Ko and Scott (1967) and (1968) and Rowe (1963a and b). Experimental results on sand indicate that loosely compacted sand will initially compact and then dilate while densely packed sand will begin to dilate almost immediately when subjected to a shearing strain.

The concept of dilatancy has been extended from the behavior of granular materials to the behavior of jointed rock masses by Goodman and Dubois (1972). Different types of joints are classified according to whether they dilate or contract when subjected to shearing strain. Again the volume change is due to relative rigid body motion of one side of the joint with respect to the other. Pore volume is either increased or decreased by the motion.

Dilatancy has also been observed by many investigators on laboratory tests on intact samples of geologic materials. Bridgeman (1949) reports on volume changes in simple compression for both rocks and metals. From his experiments, Bridgeman concludes that the volume increase is a strong function of stress and that the component of volume increase is largely reversible and recoverable on release of stress.

The volume change during plastic flow is assumed to be due to the opening or closing of interstices. Whether volume increases or decreases depends on the number of original imperfections, their size and their orientation with respect to the principal stress directions.

More recent experiments on volumetric strains in rock have been reported by Crouch (1970) who ran deformation controlled tests on Wombeyan marble, sandstone, norite, quartzite and aluminum. All of the rocks exhibited an increase in volume (dilation) beginning at about one-half the maximum axial stress. Tests on quartzite showed that confining stresses of up to 5000 lb/in^2 did not appreciably affect the axial stress-axial strain behavior beyond the peak axial stress, but considerably reduced the amount, although not necessarily the rate, of volumetric expansion.

Volume changes at strains up to 20 per cent and confining pressure up to 8 Kb have been observed by Edmond and Patterson (1972) using a dilatometric method. They note that for Gosford sandstone, compaction can be followed by dilation as straining continues. An alternate flow parameter defined as the total rate of doing work on the specimen is presented as a better guide in deducing the relative roles of cataclastic flow and intracrystalline plasticity as mechanisms of deformation.

Brace, Paulding and Scholz (1965) reported on dilatancy in the fracture of crystalline rocks. Volume changes in a granite, a marble and an aplite were measured under confining pressure up to 8 Kb. The volume change behavior, as measured by electrical resistance strain gages, was found to be similar for the rocks tested. Dilatant behavior began when the maximum stress was in the range between one-third and two-thirds of the fracture stress at the prevailing pressure. The magnitude of the dilatancy ranged from 0.2 to 2.0 times the elastic volume changes that would have occurred if the sample were simply linearly elastic. The magnitude of the dilatancy was not strongly influenced by confinining pressures in the range used. The stress at which dilatancy began was found to be dependent on the loading rate for the granite. Dilatancy was found to represent an increase in porosity due to open cracks which formed parallel to the direction of maximum stress.

Since dilatant behavior has been observed in tests of materials in the plastic range, attempts have been made to incorporate the phenomena in continuum theories of plastic flow. Drucker and Prager (1952) presented a three-dimensional generalization of the Mohr-Coulomb failure hypothesis and demonstrated that plastic deformation must be accompanied by an increase in volume for materials exhibiting

Mohr-Coulomb type behavior. The corresponding yield surface in three-dimensional stress space is a right circular cone while experiments conducted at high pressure attest to the convexity of the failure envelope. Therefore, the model developed by Drucker and Prager is representative only for moderate pressures. Nelson, Baron, and Sandler (1971) discuss four mathematical models for geologic materials used in wave-propagation studies. These models have been developed for use in large computer codes of the finite difference and finite element type employed in ground shock studies.

It is generally accepted that dilatancy phenomena whether associated with granular materials, joint movement or plastic-flow in geologic materials must be accompanied by an increase in porosity in order that mass is conserved. Whether or not the dilatancy is accompanied by an increase in permeability depends on the particular situation under consideration. For example, the dilatancy of sand is almost certainly accompanied by an increase in permeability. Dilation caused by movement along a saw-tooth type joint may or may not increase permeability depending on the degree to which the newly created voids are interconnected. The dilation of rocks due to the opening of interstices may or may not change the permeability depending on their size which, of course, depends on the amount of deformation and

the degree to which they are interconnected which also probably depends on the amount of deformation.

Scholz, Sykes and Aggarwal (1973) have recently discussed a physical basis for earthquake prediction. Rock dilatancy and water diffusion are used to explain a large class of phenomena shown to be consistent with a dilating model are premonitory changes in the ratio of seismic compressional velocity to seismic shear velocity, changes in electrical resistivity, rate of water flow (or radon emission), geodetic measurements and number of seismic events. An earthquake event is divided into six distinct stages beginning with the build up of elastic strain energy, progressing to dilatancy, followed by an influx of water, the earthquake, sudden stress drop and finally aftershocks. This model originally proposed independently by Nur (1972) and Aggarwal et. al. (1973) indicates that longer warning times should be available for larger magnitude earthquakes. The model appears to be most applicable to earthquakes involving a significant component of thrust faulting and where conditions allow large stresses to develop. The authors note "that it is possible that stresses along simple strike-slip faults such as in central California will not rise high enough to initiate dilatancy; however, the Danville earthquake, which was preceded by anomalous

tilts, had a strike-slip mechanism." This writer believes that it is a mistake to assume that dilatancy will always be accompanied by high stress levels. Dilatancy in a fractured medium is basically a geometric rigid body motion process. Consequently, an already fractured zone may undergo boundary motion parallel to the fault and dilate with relatively little stress build-up. From this, it would follow that the existence of a dilating zone may be a necessary condition for an earthquake mechanism, however it does not appear to be a sufficient condition. This view is supported by the fact that the proposed mechanism requires the existence of a pore fluid while dilatancy phenomena can exist in the dry state.

1.2 Purpose and Scope of This Study

The primary objective of this study is the investigation of dilatancy related instabilities from a theoretical point of view. This has been accomplished by first considering the nature and characteristics of mechanically unstable systems. A computerized numerical model exhibiting many of the characteristics of fluid induced instabilities has been developed and tested. Laboratory tests have been performed to study the spatial variation of dilatancy in Weber sandstone and to establish the appropriate form of the relationship between distortional deformation and volume

change.

1.3 The Nature of Instabilities

The purpose of this section is to define a primitive concept of mechanical instability and to discuss the conditions under which real systems may become unstable. Since instability is a state opposite of stability or equilibrium, we will first consider the total equilibrium of a system. In order for a system to be in total equilibrium, it must be in mechanical, thermal, chemical and electrical equilibrium. Any perturbation of the equilibrium state may cause interaction among the fields. In classical physics, phenomena in each of these categories have often been considered independently. This uncoupling is usually justified since in many practical situations, the fields are only weakly coupled. For example, the triaxial compression of a solid will raise its temperature slightly but this fact is neglected in the classical theory of elasticity and most thermo-elastic solutions are derived on the assumption that the temperature field may be computed independently of the stress field.

If the fields should be strongly rather than weakly coupled, a perturbation in one field may create a reaction in another field such that the system becomes unstable. An example of such a coupling that is relevant to seismic

instability is the development of pore pressure by the dehydration of minerals as discussed by Raleigh and Patterson (1965). In this situation, the chemical and mechanical fields are coupled and the resultant increase in pore pressure could conceivably trigger a release of stored mechanical strain energy.

An earthquake results from a sudden release of energy that manifests itself in the form of kinetic energy. Consequently, the nature of mechanical instabilities is of prime importance in understanding the basic mechanism or mechanisms. In the discussion that follows, we shall define a mechanical instability as a significant (or at least non-trivial) increase in kinetic energy that results when a system in an equilibrium state is perturbed to an adjacent state by an infinitesimal input of energy. If the tendency of the system is to return to its original state of equilibrium, the system is stable in that state. However, if the system seeks a new equilibrium state, the original state is considered to be unstable.

The basic concept of mechanical stability can be demonstrated by considering the conservative system illustrated on Fig. 1.3.1. The three systems shown consist of a ball free to roll under the influence of gravity without friction or any other dissipation on the surfaces of various

curvature. In the stable situation, we note that if the ball is moved to any adjacent kinematically admissible position, work must be done on the system and the new position is one of higher potential energy. Since the work done on the system is assumed to be infinitesimal, the increase in potential energy must also be very small. If the ball is released from its new position, it will move toward its original position and oscillate about that equilibrium position with an infinitesimal amplitude. We note that in the stable position the system has no capacity to do work, the potential energy is a minimum.

In the unstable case, any kinematically admissible movement, will result in a decrease in the potential energy. Since no energy is dissipated by the system the decrease in potential energy must be taken up by an increase in kinetic energy such that the change in kinetic energy plus the change in potential energy is constant. In this case the ball will never return to its original position which is one of maximum potential energy.

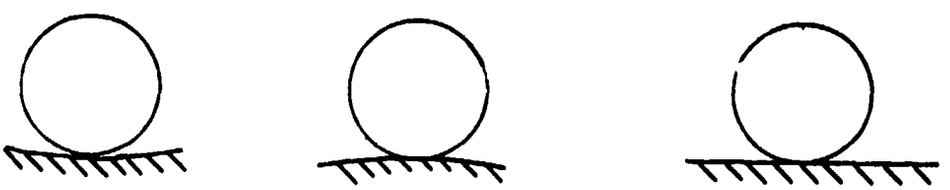

a. Stable b. Unstable c. Neutral

Fig. 1.3.1 Stability of a conservative system

In the case of neutral stability, any kinematically admissible movement will result in no change in the total potential energy of the system. An infinitesimal amount of work done on the system will be entirely converted to kinetic energy.

From the above, we conclude that for mechanically conservative systems a stable equilibrium position exists if the total potential energy of the system is a minimum. An unstable equilibrium exists if the potential energy is a maximum. This principle has been widely used in the analysis of elastic structures as well as in the basic formation of the finite element method from variational principles. Thus the principle that nature seeks states of lower potential energy is applicable in both rigid body and continuum mechanics.

All real systems are dissipative in nature and ideal conservative behavior is only approached in reality. Consequently, we must concern ourselves with the stability of systems containing dissipative mechanisms and study the role of dissipative mechanisms in stability. If we consider the ball shown on Fig. 1.3.1 to be constrained to slide on a track with no rolling, the three systems shown become non-conservative systems since the sliding friction dissipates mechanical energy into thermal energy.

In the stable case, any kinematically admissible movement requires work done on the system that is sufficient to overcome the mechanical energy dissipated by friction and increase the potential energy. Since the system is perturbed only by an infinitesimal work input, we conclude that the stability of equilibrium of the system is not changed by the presence of a dissipative mechanism.

The situation is not quite so simple for case b, the previously unstable case. If we consider a perturbation to an adjacent kinematically admissible state, conservation of mechanical energy, as derived in Appendix I, requires that

$$\Delta KE + \Delta PE = {}_1W_2 + {}_1W_2^f = {}_1W_2 - \left| {}_1W_2^f \right| \qquad (1.3.1)$$

where ΔKE and ΔPE represent changes in kinetic and potential energy respectively and ${}_1W_2$ equals the infinitesimal positive external work done on the ball while ${}_1W_2^f = -\left| {}_1W_2^f \right|$ is the work done by friction which opposes the motion. Since the mechanical work done by friction is negative, it is written as a minus sign times the absolute value in order to emphasize the point.

Since the criterion for mechanical stability has been stated in terms of changes in kinetic energy, Eq. 1.3.1 may be rewritten as

$$\Delta KE = {}_1W_2 + {}_1W_2^f - \Delta PE \qquad (1.3.2)$$

Three situations are now possible, if $\Delta PE = {}_1W_2^f$ we have

$$\Delta KE = {}_1W_2 = \varepsilon \qquad (1.3.3)$$

where

$$0<\varepsilon<<1$$

This is essentially the case of neutral stability since the work of perturbation is assumed to be negligibly small.

If $\delta = \Delta PE - {}_1W_2^f > 0$, which implies that $|\Delta PE| < |{}_1W_2^f|$, (since both terms are less than zero) in this case, then Eq. 1.3.2 becomes

$$\Delta KE = \varepsilon - \delta \geq 0 \tag{1.3.4}$$

where we require that ΔKE is greater than or equal to zero since $KE_1 = 0$ which implies that

$$\Delta KE = KE_2 = \tfrac{1}{2}mv_2^2 \geq 0 \tag{1.3.5}$$

The situation implied by Eq. 1.3.4 is clearly impossible since ε is negligibly small and δ was postulated as being greater than zero, but not necessarily small. Stated in words, the postulated situation requires that more energy be dissipated than is available from the change in potential energy plus the infinitesimal external work done on the ball. It follows then that an inherently unstable state in the absence of a dissipative mechanism can become stable in the presence of a sufficient dissipative mechanism.

A third situation exists if $\beta = {}_1W_2^f - \Delta PE > 0$. Then Eq. 1.3.2 becomes

$$\Delta KE = \varepsilon + \beta > 0 \tag{1.3.6}$$

Since both ε and β are always greater than zero, the situation always results in a nontrivial increase in kinetic energy and we have an inherently unstable state. We conclude that the presence of a dissipative mechanism is not suffi-

cient to always insure stability.

The equals sign shown in both Eq. 1.3.4 and 1.3.5 coincide with the case of Eq. 1.3.3 which is essentially neutral stability. This implies that the neutrally stable situation exists as a transition between inherently stable and unstable states.

To summarize the stability analysis, we may write

$$(\Delta PE - {}_1W_2) \begin{cases} > {}_1W_2^f = -|{}_1W_2^f|, & \text{Impossible, state 1 stable} \\ = {}_1W_2^f = -|{}_1W_2^f|, & \text{Neutral} \\ < {}_1W_2^f = -|{}_1W_2^f|, & \text{Unstable} \end{cases} \tag{1.3.7}$$

which holds even if the reversible work done between 1 and 2 is nontrivial. It should be noted that Eq. 1.3.7 holds also for the conservative case previously discussed where ${}_1W_2^f = 0$. Eq. 1.3.7 can be further generalized to

$$|\Delta PE - {}_1W_2| \begin{cases} < |{}_1D_2|, & \text{Stable} \\ = |{}_1D_2|, & \text{Neutral} \\ > |{}_1D_2|, & \text{Unstable} \end{cases} \tag{1.3.8}$$

where ${}_1D_2$ represents total mechanical energy dissipated by all mechanisms is the transition of the system from state 1 to state 2.

The mechanical energy dissipation term, D, is often more easily expressed as a time rate, for example: when the mechanism is viscous in nature, or the coefficient of friction is time dependent as suggested by Dieterich (1972). The appropriate form of Eq. 1.3.8 then becomes

$$|\dot{PE}-\dot{W}| \begin{cases} <|\dot{D}|, \text{ Stable} \\ =|\dot{D}|, \text{ Neutral} \\ >|\dot{D}|, \text{ Unstable} \end{cases} \qquad (1.3.9)$$

where $\dot{W}$, $\dot{PE}$, and $\dot{D}$ are respectively the time derivatives of reversible work, potential energy and the dissipation function.

So far we have considered only the conservation of mechanical energy which is simply the first integral of the conservation of linear momentum and must always be satisfied. The other conservation laws of physics must also be satisfied and provide further insight into the general nature of instabilities. Conservation of mass has already been mentioned in connection with dilation caused by rigid body motion between grains or blocks. Conservation of total energy, essentially the first law of thermodynamics, provides us with the means to link the mechanical, thermal, chemical and electrical fields. It further allows the computation of these associated fields when the appropriate consitutive equations and equations of state are specified. Our primary interest in the associated fields is the possibility that a change in one or more of these coupled fields could precipitate a mechanical instability resulting in the sudden release of a substantial amount of energy in the form of kinetic energy. Any such interaction between fields must satisfy the first law of thermodynamics in its most general form.

The second law of thermodynamics requires that the

change in entropy (for the system plus its surroundings) between two states must be greater than or equal to zero. The change in entropy of the system plus its surroundings can only approach zero for real systems since a zero change in entropy implies a conservative process. The second law of thermodynamics places restrictions on processes which insure that they are actually physically possible. This can be an important point in the design of numerical models of processes such as seismic instability.

The role of the laws of thermodynamics can be clarified by again considering the problem shown on Fig. 1.3.1 where the ball is constrained to slide and there is dissipation of mechanical energy due to friction. Conservation of mechanical energy of the ball may be written in differential form as

$$d(KE+PE)=dw+dw^f=dw-|dw^f| \qquad (1.3.10)$$

The appropriate form of the first law of thermodynamics for a system of ball plus track may be expressed as

$$d(U+KE+PE)=dw-dw^f+dQ=dw+|dw^f|+dQ \qquad (1.3.11)$$

where U is the internal energy function and dQ is the differential heat transferred into the system through the boundaries as the ball slides. The work term, dW, in both Eqs. 1.3.10 and 1.3.11 is presumed to be reversible work that is not dependent on the path taken while dW^f is differential frictional work and is dependent on the path. Note that Eq. 1.3.10 considers only the ball as the system. If we subtract Eq. 1.3.10 from 1.3.11, we have

$$dU = -2dW^f + dQ \tag{1.3.12}$$

For a reversible process, $dW^f=0$ and $dS = dQ/T$ where S is entropy and T is the absolute temperature. Substituting these relations into the first law of thermodynamics yields

$$TdS+dW=d(U+KE+PE) \tag{1.3.13}$$

which must hold for both reversible and irreversible processes since the equation is entirely in terms of properties of the system and the reversible work, dW, done on the system.

Substituting Eq. 1.3.12 into 1.3.13 gives

$$TdS+dW=2dW^f+dQ+d(KE+PE) \tag{1.3.14}$$

If we now substitute for d(KE+PE) from Eq. 1.3.10, we have

$$TdS = dQ - dW^f = dQ + |dW^f| \tag{1.3.15}$$

But

$$dS = \frac{dQ}{T} + d\phi \tag{1.3.16}$$

which states that the differential change in entropy of the system equals differential entropy transported into the system by heat plus the differential entropy generated within the system, $d\phi$. The differential entropy generated within the system must be greater than or equal to zero, hence

$$d\phi > 0 \tag{1.3.17}$$

If we eliminate dS from Eqs. 1.3.15 and 1.3.16, we have

$$d\phi = -dW^f = |dW^f| > 0 \tag{1.3.18}$$

Now the differential work done by friction is

$$dw^f = -\mu N d\xi \tag{1.3.19}$$

where μ= coefficient of friction, N is the normal force, ξ is a position coordinate, and motion is assumed to be in

the positive ξ direction ($d\xi>0$). If we substitute into Eq. (1.3.17),

$$d\phi = \mu N d\xi \geq 0 \tag{1.3.20}$$

Since N and $d\xi$ are postulated to be ≥ 0, we must have

$$\mu \geq 0 \tag{1.3.21}$$

in order not to violate the second law of thermodynamics. This is hardly a startling result but is typical of the restrictions placed on processes by the second law of thermodynamics. The second law essentially prohibits the existence of perpetual motion machines and is a statement of common experience. In more complex models, restrictions are not always so obvious and the second law provides a formal way to analyze a given process.

Stability investigations are sometimes made by employing Gibb's free energy (referred to as free enthalpy). Murrell and Digby (1972) consider the thermodynamics of brittle fracture initiation under triaxial stress conditions by using Gibb's free energy. Gibb's free energy also provides us with a link to the stability of interacting processes involving mechanical, chemical, thermal and electrical fields. Gibb's free energy is a thermodynamic potential function defined in terms of state variables as

$$G = H - ST \tag{1.3.22}$$

where H is the enthalpy of the system, S is the entropy and T is the absolute temperature. In Eq. 1.3.22 the enthalpy, in the most general case, is defined as the internal energy minus the summation of the product of the thermodynamic

tensions and their conjugate substate variables. The thermodynamic tensions and conjugate substate variables may have mechanical or electromagnetic dimensions as discussed in Malvern (1969). Chemical potentials also are related to Gibb's free energy as discussed in Denbigh (1968).

There is much information available on the thermodynamics of continuum processes as summarized by Malvern (1969) where the original references may be found. Since a dilatancy related instability is not necessarily a continuum process, we have chosen to work from first principles in investigating the basic nature of instability. The results of this phase of the investigation may be summarized as follows:

1) The primary criterion for mechanical instability is a non-trivial increase in kinetic energy resulting when an equilibrium state is perturbed by an energy input of negligible magnitude.

2) In a conservative system, a stable equilibrium configuration is characterized by minimum total potential energy.

3) An equilibrium state of other than minimum total potential energy can be stable in the presence of a dissipative mechanism such that $|\Delta PE| < |{}_1D_2|$ for an infinitesimal, kinematically admissible perturbation from state 1 to state 2.

4) The presence of a dissipative mechanism alone does not insure the mechanical stability of an inherently

unstable system. For stability, the dissipation must be of the magnitude such that the inequality stated in 3 above is satisfied.

5) Any real, physically possible process must result in an increase in entropy of the system plus its surroundings, i.e., states of higher entropy are preferred by nature.

6) Mechanical, thermal, chemical and electrical (electromagnetic) fields are coupled by the most general statement of conservation of energy. A perturbation in any one of these fields may cause a system with some potential energy to become mechanically unstable. In this situation, it may be convenient to use a stability criterion involving Gibb's free energy.

1.4 Frank's Model-Dilatancy Instability

Frank (1965) proposed a seismic instability model involving dilatancy of a system of non-uniform, rigid body grains and frictional dissipation of mechanical energy. The relationship between volume change and shearing displacement was assumed to be that shown of Fig. 1.4.1 for a well-packed but only statistically regular system of non-uniform grains. Stated in words, the criterion used by Frank for instability is

Work done on the system	-	Work done by the system	>	Energy dissipated by friction

In equation form, we have

$$\tau d\gamma - (P-P_i)m d\gamma > \tau_f d\gamma \qquad (1.4.1)$$

where τ is the overall shear stress, $d\gamma$ is the differential

movement, P is the total pressure, P_i is the pressure in the interstitial fluid which is assumed to be in communication with a reservoir, m is the slope of the volume change versus displacement curve shown on Fig. 1.4.1, and τ_f is the frictional stress. Assuming that the frictional stress is proportional to $(P-P_i)$ gives

$$\tau_f = n(P-P_i) \tag{1.4.2}$$

where n is an appropriate coefficient of friction. Combining Eqs. 1.4.1 and 1.4.2 gives

$$\tau > (P-P_i)(m+n) \tag{1.4.3}$$

as the criterion for further slip. The point at which slip is imminent is

$$(P-P_i)_c = \tau/(m+n) \tag{1.4.4}$$

where the subscript c has been added to indicate that this is the critical state. If $(P-P_i)$ becomes less than $(P-P_i)_c$ slip will occur. Consequently, as long as $dm/d\gamma$ is greater than zero, the situation is essentially stable since any movement $d\gamma$ will increase m and decrease the right hand side of Eq. 1.4.4. If γ increases beyond the inflection point shown on Fig. 1.4.1, $dm/d\gamma$ becomes negative and any further increase in displacement leads to a decrease in m which increases the right hand side of Eq. 1.4.4, thus requiring a larger value of $(P-P_i)$ to maintain stability.

1.5 Comments on Frank's Model

From the above discussion of Frank's model, it is evident that the point of inflection of the volume change versus displacement curve is critical to the existence of

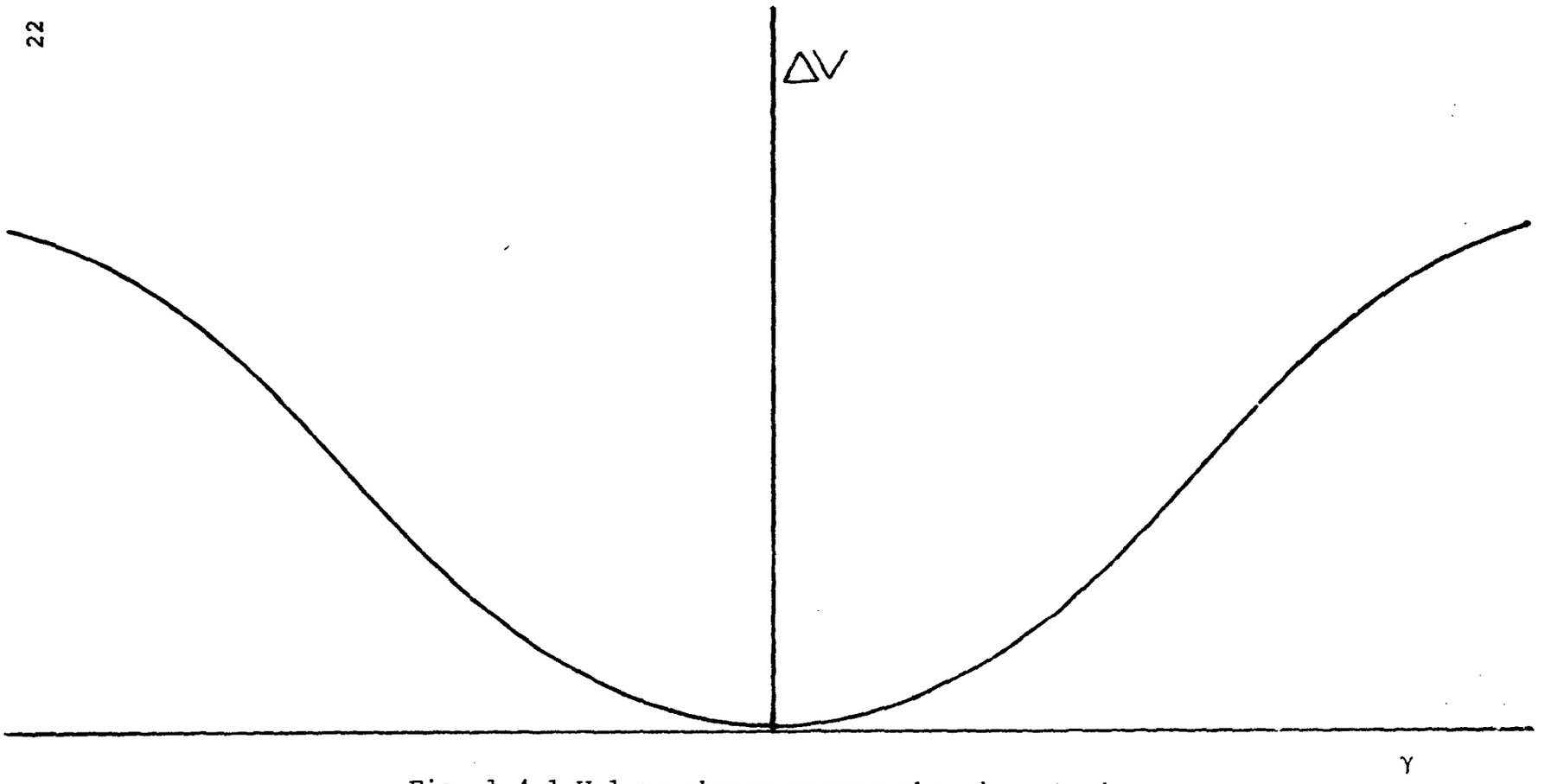

Fig. 1.4.1 Volume change versus shearing strain

the mechanism. Experimental results reported by Brace, Paulding and Scholz (1966) do not indicate such an inflection point for the rocks studied. Results presented in section 3 of the present report indicate that a change in curvature is possible at least at some point on a test sample.

Orowan (1966) discussed Frank's model and concluded that the implicit assumption that the coefficient of friction remained constant during the movement was impossible. Furthermore, Orowan concluded that the instability attributed to dilatancy is a familiar general property of compacted granular masses independent of whether or not the mass dilates. Orowan states, "the deformation of a consolidated granular mass is mechanically unstable; this circumstance is a dominating fact of soil mechanics, responsible for most slope failures and landslides and some avalanches." Orowan also states that, "Dilatancy, if present, influences only the effective pressure ($P-P_i$) but does not create any specific instability."

Neither Frank nor Orowan discusses the possibility that the total pressure, P, may also depend on the displacement, γ. This situation would appear to be likely when an existing fault zone is undergoing a shearing displacement and hence subject to dilation. As a first approximation, we may assume that the pressure, P, is related to the shearing displacement in an idealized situation as shown on Fig. 1.5.1. In this case, the

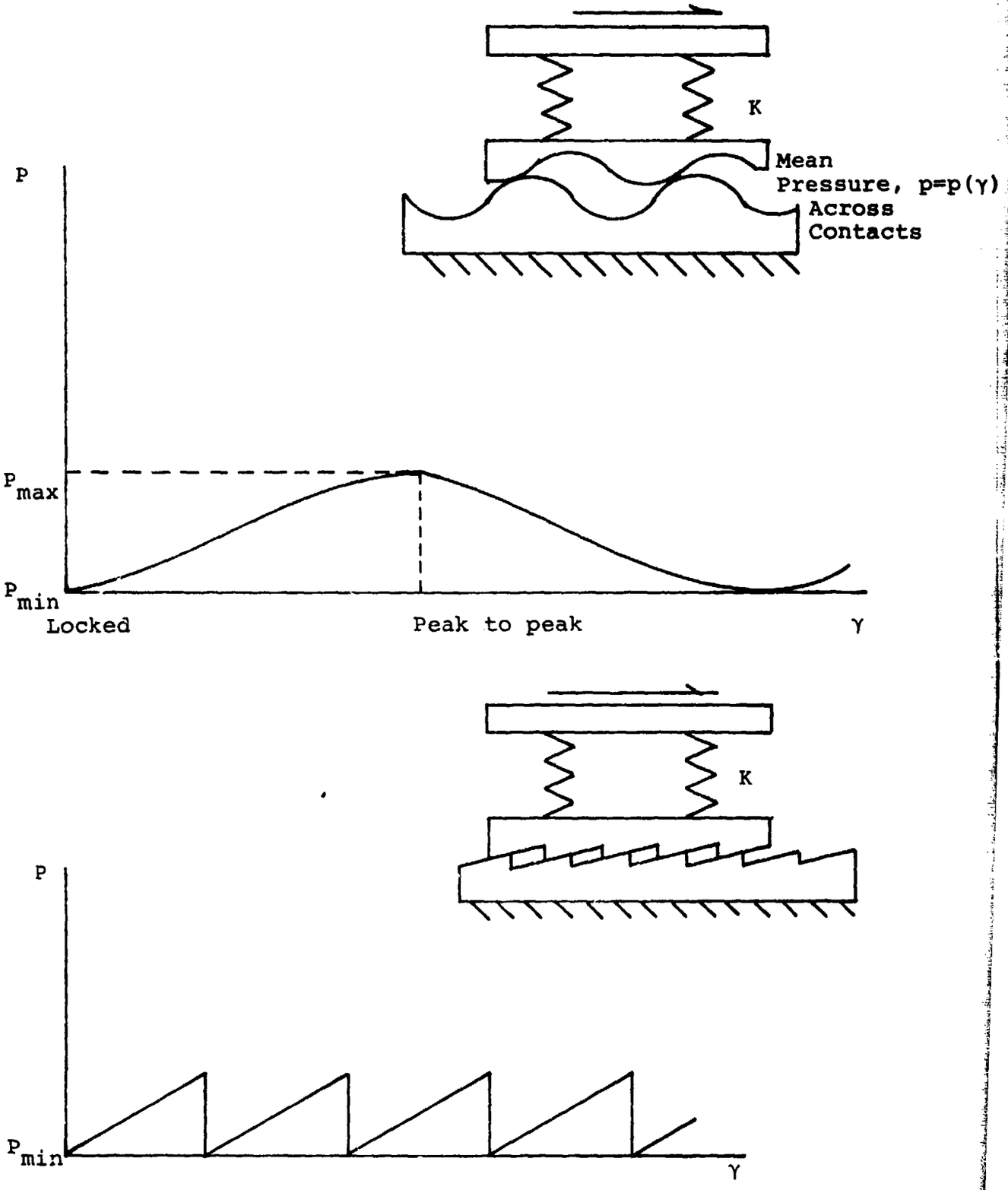

Fig. 1.5.1 Intergranular pressure as a function of displacement

asperities are assumed to be rigid but on the face of an elastic mass. The motion is presumed to be dominately rigid body in nature. The effect indicated would probably not be important in slope failures or any problems where there is insufficient constraint to develop the increased pressure. On the other hand, if the pressure is large enough that the frictional force between the faces exceeds the shearing strength of the asperities, new fractures may develop and the shear zone may become larger. It is interesting to note that this mechanism reinforces dilatancy hardening since, in the idealized cases shown, the peak total pressures coincide with the maximum increase in pore volume and consequent decrease in P_i. Both mechanisms act to increase the effective stress, $(P-P_i)$.

Eq. 1.4.1 implies that all the energy input into the system must be dissipated by friction if the system is to be stable. In reality, some of the net work done on the system may be stored as potential energy probably in the form of strain energy. It is this stored potential energy that is generally thought of as the source of the kinetic energy released during an earthquake.

2. NUMERICAL STUDY OF DILATANCY RELATED INSTABILITY

2.1 Introduction

The primary objectives of the numerical phase of this study is to illustrate with a one-dimensional, (1-D), lumped parameter model the possible coupling between the pore fluid and solid regimes may take place through 1) the effective stress concept and 2) the relationship between dilatancy and pore fluid pressure. External fluid injection or withdrawal is directly related to pore pressure and consequently effective stress as demonstrated by the Rangely experiments. The relative importance of dilatancy coupling in a fluid injection situation may be smaller than in a situation where the fault zone is loaded by plate motion. The 1-D model developed below incorporates both types of coupling.

A second objective of the numerical study is to demonstrate that the response of the fault zone may take the form of stable sliding (creep) or wave propagation (an earthquake event) depending on the rate of energy input to the system and the dissipative characteristics of the system. The model also demonstrates the diffusion of locally high pore pressures through the system.

The third objective of the numerical study is to relate instability in the model to the energy rate criterion developed in Section 1.

2.2 Development of a Model

A one-dimensional model has been chosen 1) for ease in formulation, 2) for the relatively small amount of

computer time required, and 3) since it exhibits qualitatively the characteristics of more complex and expensive models. The one-dimensional model has the disadvantage that it is difficult or impossible to obtain meaningful quantitative results or even to assign relatively consistent values to the parameters. It does, however, represent a first step in modeling a very complex coupled mechanical-fluid system.

Previous work has been done on lumped parameter, one-dimensional models of fault zones by Burridge and Knopoff (1967) and Dieterich (1972). Both of these models are comprised of a system of rigid blocks interconnected by springs, and sliding with friction on a surface. The model developed here places each rigid mass in a container with fluid.

The basic element is shown on Fig. 2.2.1 where detail of frictional surface is shown.

This basic element is similar to that used by Dieterich except for the assumptions that

1) Each mass is in a container that will hold fluid and the containers are connected by pseudo "pipes" with characteristics that can vary between elements.

2) The asperities on the frictional surface cause the pore volume to change when the mass moves thus causing the pore pressure to fluctuate. This pressure fluctuation, along with effective stress, couples the fluid motion with the block motion.

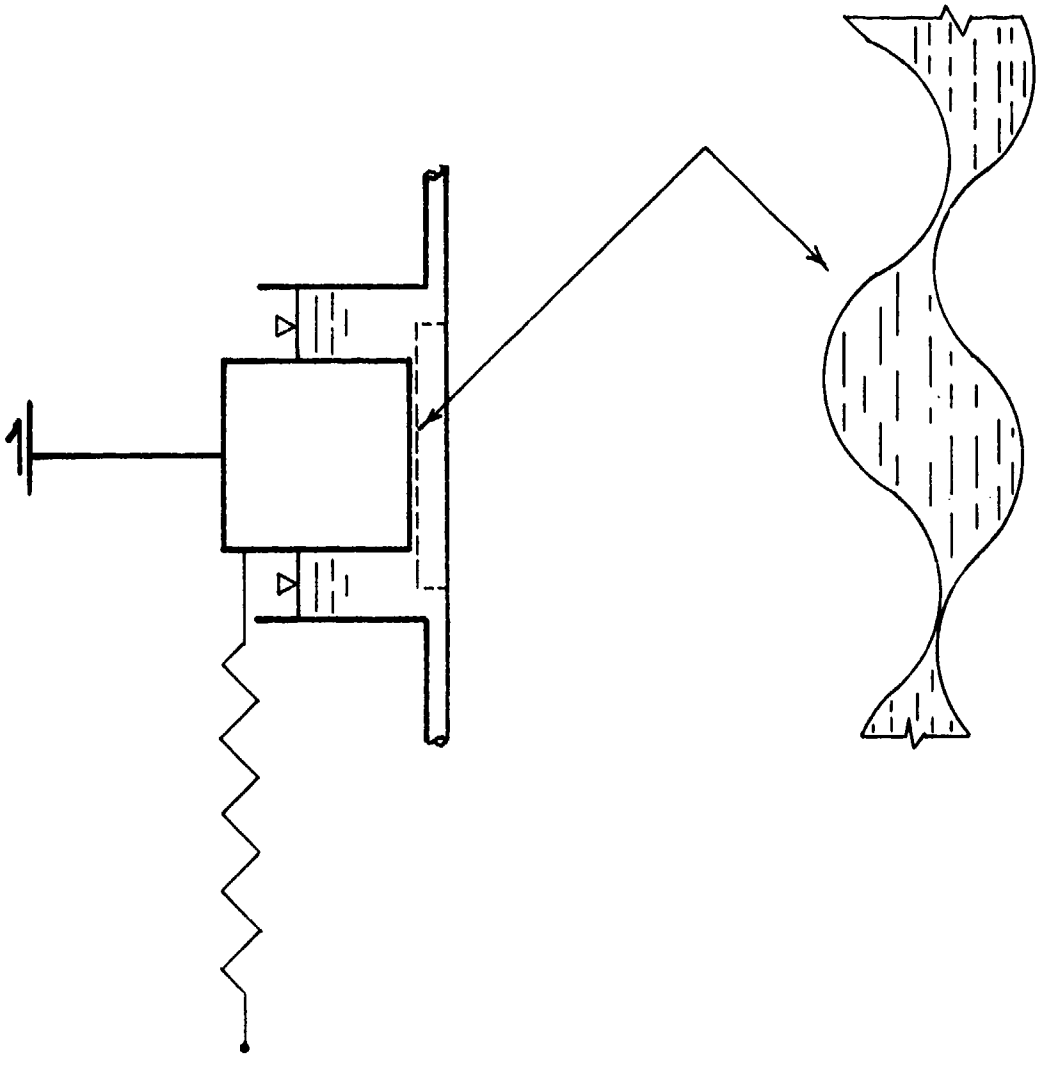

Fig. 2.2.1 The basic element

3) Fluid may be injected or withdrawn from any element so that Rangely type experiments can be conducted.

4) The rigid bar at top of lief springs is not moving with constant velocity as in Dieterich's model but the top anchor on any lief spring may be displaced to preload the model.

Three types of equations are required to describe the motion of the system. These equations are a) a momentum equation for each block mass, b) a momentum equation for the fluid in each "pipe" and c) a continuity (conservation of fluid mass) equation at each block. The momentum equation for a typical block may be written as

$$\frac{dVi}{dt} = \frac{1}{M_1}\begin{cases} 0; V_i=0 \text{ and } |F_{ie}|<|F_{if}| \\ F_{ie}-F_{if}; \text{ otherwise} \end{cases} \qquad (2.2.1)$$

where

V_i = the velocity of block "i"

t = time

M_i = mass of block "i"

F_{ie} = the elastic force exerted on block "i" by the coil and lief springs, or

$$F_{ie} = \sum_{j=i-1}^{j=i+1} K_{ij}X_j + K_i^1 X_i^o \qquad \text{where}$$

K_{ij} = force on block "i" due to a unit displacement at j with all other displacements equal to 0.

X_j = displacement of block "j"

X_i^o = original displacement of top anchor of lief spring at "i"

K_i^1 = stiffness of the lief spring at block "i"

$$F_{if} = \begin{cases} Sgn(F_{ie})\left[C_i + \mu_{si}(P_i - \gamma h_i)\right]; v_i = 0 \\ Sgn(V_i)\ \mu_{di}(P_i - \gamma h_i)\ ; v_i \neq 0 \end{cases}$$

where $Sgn(y) = \begin{cases} +1; & y>0 \\ 0; & y=0 \\ -1; & y<0 \end{cases}$

C_i = cohesion at block "i"

μ_{si} and μ_{di} = respectively static and dynamic coefficients of friction

P_i = pressure on block "i"

γ = specific weight of the fluid

h_i = fluid head in container "i"

The displacement of block "i" may be calculated from the relationship

$$\frac{dXi}{dt} = V_i \qquad (2.2.2)$$

It should be noted that the velocity and displacement of block "i" are coupled with the motions of all of the other blocks in the system through the stiffness matrix K_{ij}. Also, the motion of block "i" is coupled with the fluid motion in the system through the fluid head term that occurs in the effective stress.

The fluid motion in the "pseudo pipes" is assumed to be "plug" flow, i.e., the fluid mass in a pipe is assumed to be incompressible and to move as a unit or plug. The momentum equation governing the fluid motion in pipe "i" may be written as

$$\frac{dUi}{dt} = -g(h_i - h_{i-1})/L_i - \lambda_i U_i |U_i| \qquad (2.2.3)$$

where

U_i = mean velocity of the fluid "plug" in pipe "i"

g = acceleration of gravity

L_i = length of pipe "i"

λ_i = a friction factor term for fluid flow in pipe "i"

Eq. (2.2.3) represents the fluid motion in a pipe in the simplest manner possible that still exhibits coupling with the block motions through the head terms and energy dissipation (damping) through the pipe friction term. The fluid model chosen is capable of representing oscillatory motions if $\lambda_i = 0$, damped oscillatory motions if λ_i is relatively small and diffusion with no oscillation if λ_i is relatively large.

The fluid motions in the pipes are related to each other by the conservation of fluid mass in each container. For a typical container "i", conservation of mass may be expressed as

Mass Flow Rate In - Mass Flow Rate Out = Mass Stored per Unit Time or

$$Q_{ip} + A_i U_i - A_{i+1} U_{i+1} = \alpha_i \frac{dhi}{dt} \qquad (2.2.4)$$

where

Q_{ip} = volume flow rate injected into container "i" by an external pump plus the rate of change of fluid volume stored due to dilation. If fluid is pumped out of the container, Q_{ip} is negative.

A_i = cross-sectional area of pipe "i"

α_i = cross-sectional area of container "i"

The pipes at both ends of the model are assumed to be connected to a reservoir that remains at a constant head throughout the motion of the models.

If the number of masses is N_m, we have

N_m momentum equations for blocks

N_m displacement-velocity equations for blocks

N_m+1 fluid momentum equations in the pipes

N_m conservation of fluid mass equations in the containers

$4N_m+1$ = total number of first order, ordinary, differential equations.

This system of differential equations may be solved numerically by a number of different methods. The fourth order Runge-Kutta-Simpson method was chosen here due to its availability and simplicity. No attempt was made to solve the equations analytically due to the nonlinear character of Eq. (2.2.3).

2.3 Characteristics of the Model

The characteristics of the model may be demonstrated by the three block system shown on Fig. 2.3.1. Potential energy is initially stored in the system by setting the values of x_i^o to non-zero values, thus preloading the lief springs. This preload is kept small enough so that no block will initially break loose and begin to move, i.e., the blocks are initially at rest.

Each container is assumed to have a head of fluid equal to the reservoir head. The fluid is assumed to be at rest.

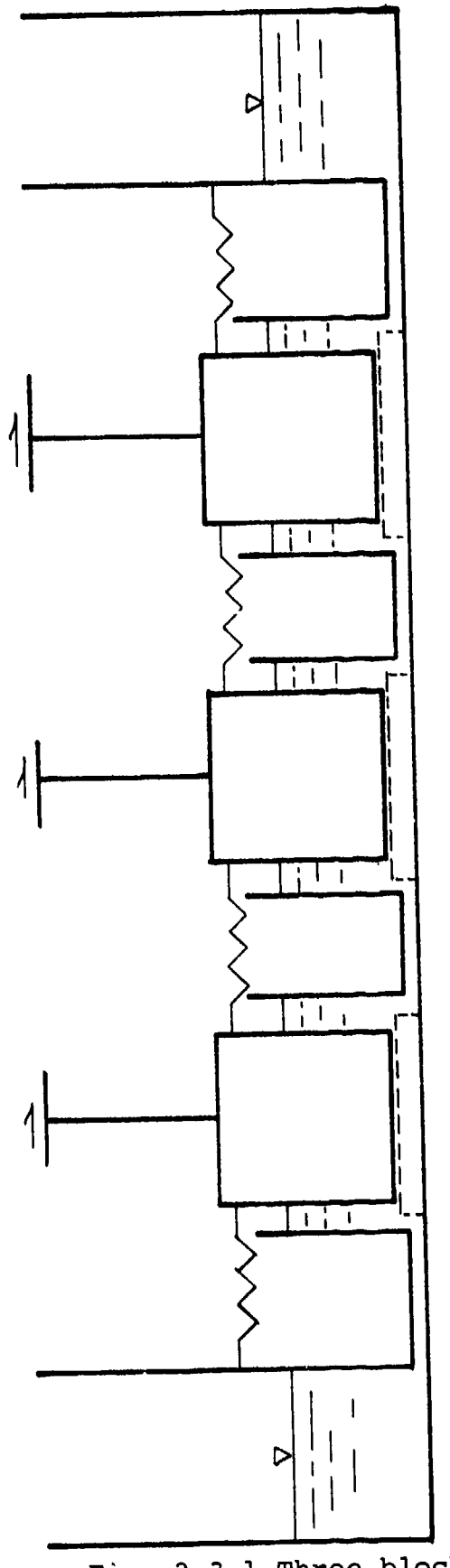

Fig. 2.3.1 Three block system

With the above initial conditions, the system is initially in equilibrium. Due to the presence of the non-zero potential energy, however, the system may not be stable. The potential energy in the lief springs is analogous to the strain energy stored in the elastic region surrounding a fault zone.

The system is now perturbed by injecting fluid into the center container as a function of time as shown on Fig. 2.3.2.

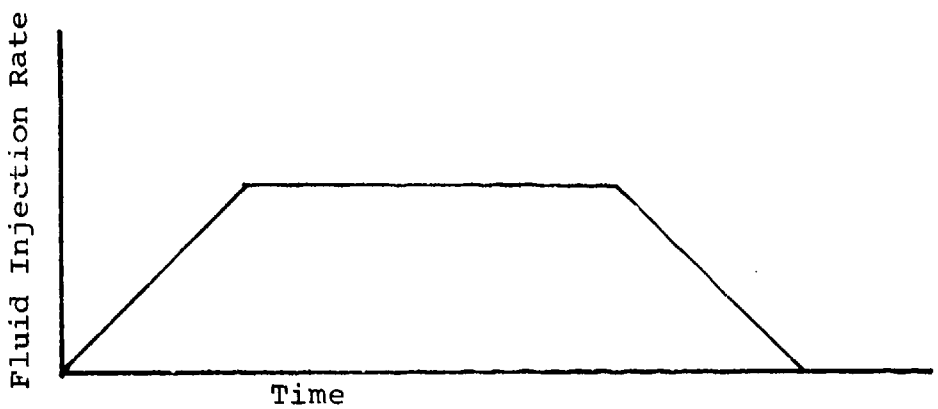

Fig. 2.3.2 Fluid injection history

As the fluid is injected into the center container, the fluid head in this container begins to rise and the system responds in one of the following ways depending on the parameters chosen.

a) If the effective stress remains sufficiently high in all of the blocks, the fluid will simply flow from the center container to the outer containers and into the reservoir. If the pipe friction is sufficiently high, the response will be simply a diffusion of the fluid pressure

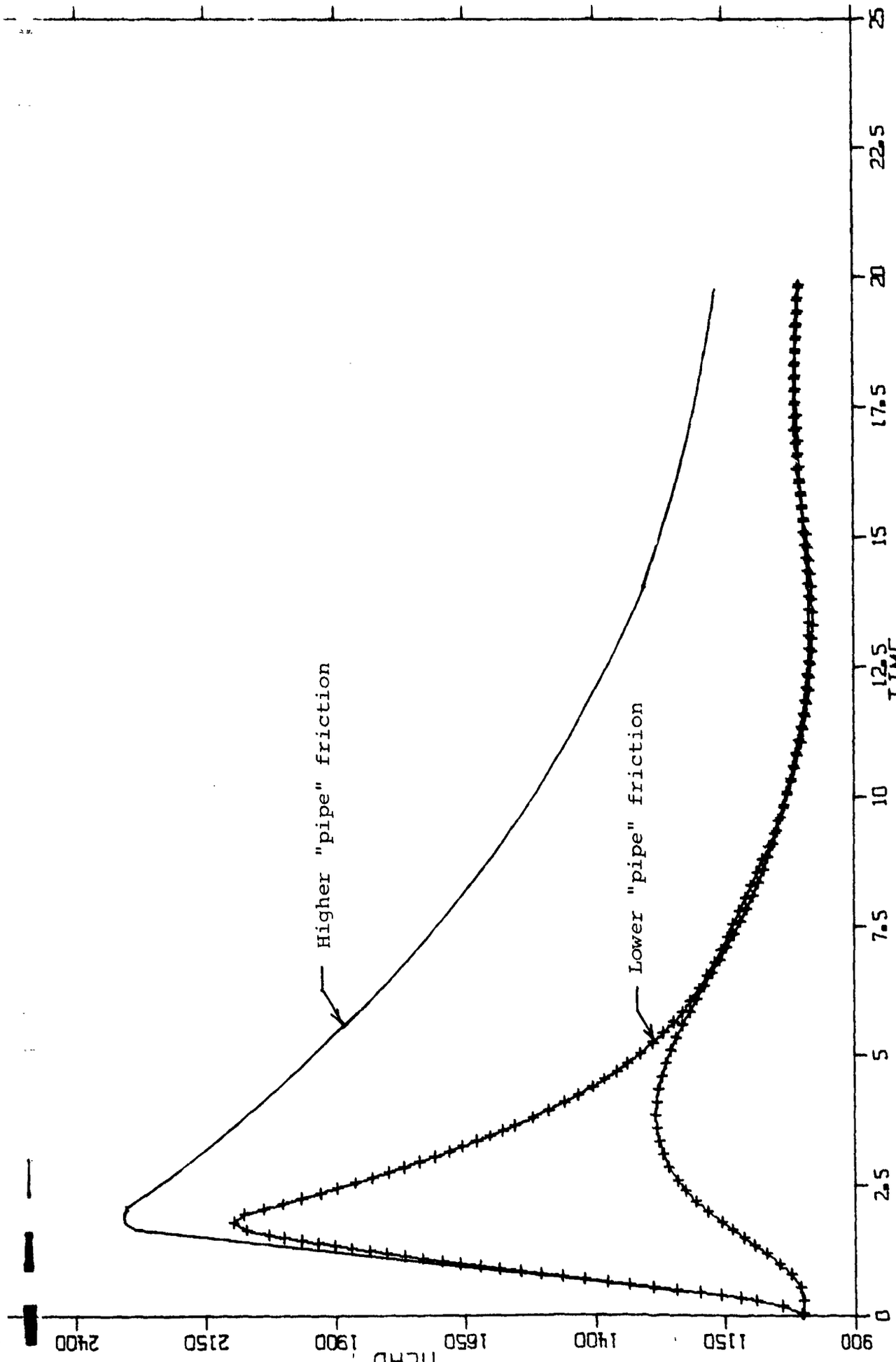

Fig. 2.3.3 Effect of "pipe" friction on hydraulic head

along the model and no oscillation of the fluid pressure will result. If the pipe friction factors are lower, the fluid motions may be of the damped oscillatory type but the blocks will remain at rest. In either case, the fluid velocities will approach zero after the injection ceases due to the dissipation of energy in pipe friction. These cases are illustrated on Fig. 2.3.3. Fig. 2.3.4 illustrates the diffusion of the head from the center to the outer container. The difference in the time of the peak heads in the containers depends on the pipe characteristics chosen.

b) If the increased fluid pressure in the center container reduces the effective stress to a sufficiently low level, the center block may break loose and begin to slide. The movement of the center block loads its leading and trailing coil springs and may cause (along with the increase in fluid pressure) one or both of the outer blocks to begin to slide depending on the strength parameters chosen. If the sliding block friction is high enough, the block(s) may simply slide slowly to a new equilibrium position with no oscillation. This is interpreted as a creep event since the dissipation of energy is relatively slow. Dilatancy hardening may occur since block motions may cause the fluid pressure to drop.

If the block friction is relatively lower, one or more of the blocks may begin to oscillate. The rapid oscillation of a mass is interpreted as an earthquake event. Both

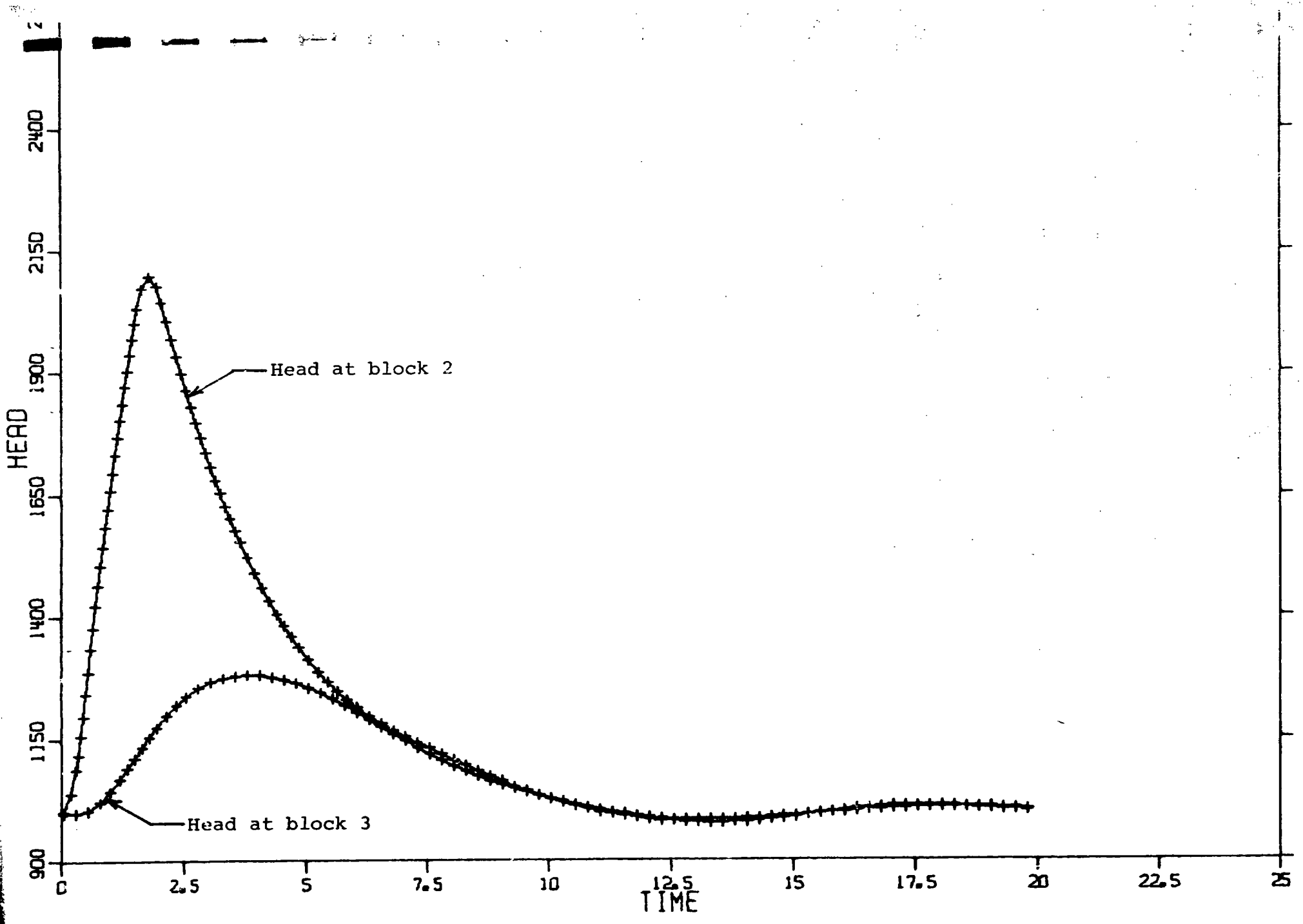

Fig. 2.3.4 Diffusion of hydraulic head

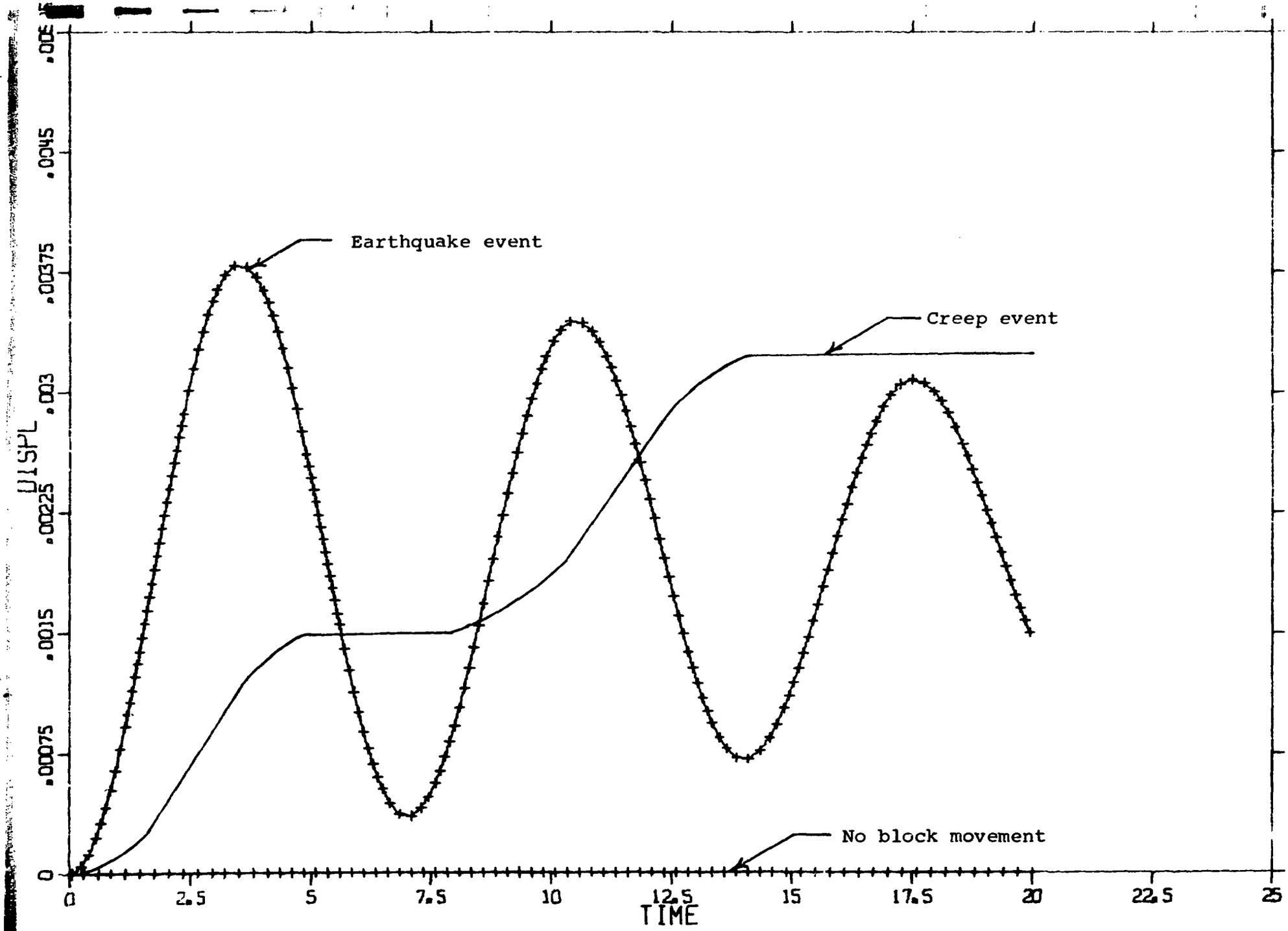

Fig. 2.3.5 Block displacement history

creep and earthquake events are illustrated on Fig. 2.3.5.

Due to the one-dimensional character of the model, an oscillating block can radiate energy only along the model and not in all directions as would occur in the earth. Another limitation of the present model is that the end blocks are connected by coil springs to fixed boundaries, thus, reflections will occur. Dieterich (1972) made his model circular in nature so that the boundary reflections could not occur. This feature could be incorporated into the present model.

Although not illustrated by the three block example, the model does allow for the possibility after shocks. A block that has come to rest after an event may again break loose and begin to oscillate.

2.4 Summary of Model Capabilities

The present model may be used to study systems having a maximum of 50 blocks with 51 pseudo pipes all having different characteristics. Coupling of the fluid and block motions due to an increase in pore pressure which reduces the frictional resistance to block movement or block movement that changes the fluid pressure due to dilatancy can be demonstrated by the model. The block response may be either creep or vibration while the fluid response may be oscillatory, damped oscillatory or critically damped (diffusion).

3. LABORATORY INVESTIGATION

3.1 Introduction

The primary purpose of the laboratory tests performed was to study the spatial variation of dilatancy in Weber sandstone and to establish the appropriate form of the relationship between distortional deformation and volume change. Previous investigators, Brace, Paulding and Scholz (1965) and Crouch (1970), have used experimental methods that assumed a uniform distribution of dilation throughout the rock core being tested. Brace, Paulding and Scholz (1965) used four electrical resistance strain gages, two parallel and two transverse, to the axis of the sample. The ratio of gage length to sample length approached unity. It is well known that for small strains,

$$\frac{\Delta V}{V_o} = \varepsilon_v + \varepsilon_t + \varepsilon_r \qquad (3.1.1)$$

where V_o = original sample volume, ΔV = change in volume, and ε_v, ε_t, ε_r are respectively the components of normal strain in the vertical, tangential and radial directions. Assuming that the sample deforms as a right circular cylinder,

$$\varepsilon_r = \varepsilon_t \qquad (3.1.2)$$

and Eq. (3.1.3) becomes

$$\frac{\Delta V}{V} = \varepsilon_v + 2\varepsilon_t \qquad (3.1.3)$$

If extension is taken as positive, the vertical strain is negative while the tangential strain is positive for uniaxial and triaxial tests. Thus calculation of the volumetric

strain involves taking the difference between the magnitude of the vertical strain and twice the magnitude of the horizontal strain, a process that can lead to erroneous results unless the strains are measured to a sufficient number of significant digits.

If a linear elastic material model is chosen as a first approximation,

$$\varepsilon_t = -\nu\varepsilon_v \tag{3.1.4}$$

where ν is Poisson's ratio and

$$\frac{\Delta V}{V_o} = (1-2\nu)\,\varepsilon_v \tag{3.1.5}$$

Since ν is always less than or equal to 0.5 for a linear elastic material, we expect that the volume of the sample should decrease as long as the linear elastic model is approximately correct since ε_v is negative. As shown later, an initial decrease in volume was observed in all samples tested.

Crouch (1970) used a hydraulic system to measure volume changes of samples. Again it is assumed that the volume change occurs uniformly throughout the sample, i.e., the shape of the sample remains a right circular cylinder that is shorter in length and larger in diameter.

If we assume that failure will develop on a plane inclined at some angle with the maximum principal stress direction, then it follows that the components of strain in the neighborhood of the failure plane will differ from the average strain in the sample as failure is approached.

Stated another way, as failure is approached, the strain field is expected to become inhomogeneous. This leads us to the assumption that much of the observed total increase in volume may in fact be concentrated in the failure zone.

In order to study this possible effect experimentally, a "whole field" method of deformation measurement appears to be the obvious choice. However, to the writer's knowledge, no such measurement technique is readily available for studying deformation in the triaxial test. Consequently, it was decided to attempt to study the distribution of strain by using a number of smaller electrical resistance strain gages to sample the strain field at a number of points on the specimen. In addition, a hydraulic system has been used to measure the average volume change of sample. This combination of techniques allows us to determine when the deformation at any given point deviates from the average.

3.2 Rock Characteristics

The principal rock chosen for the testing program was Pennsylvanian age Weber Sandstone collected from outcrops in Sheep Creek Canyon just west of the Manila Quadrangle near Utah State Highway 44. Hansen and Bonilla (1956) mapped the Manila quadrangle and described the Weber Sandstone as being a pale, yellowish-gray, fine-to medium-grained, very thickly bedded to massive cross-bedded sandstone that is well cemented. Some of the Weber Sandstone outcropping in Sheep Creek Canyon is weathered to the point where hand specimens can be readily disintegrated. An

attempt was made to collect only relatively unweathered blocks.

The Weber Sandstone was initially chosen since the experiments at Rangely were conducted in this rock. A visual comparison of the samples collected with core cut at Rangely indicated that the core was better cemented and probably less permeable than the sandstone from the outcrop.

A limited number of tests were also run on a Cambrian age sandstone from the Deadwood formation in the Black Hills. Blocks of this rock were collected from an abandoned mine in the west central part of the Black Hills near Ditch Creek. The material is referred to as Ditch Creek Sandstone and is a yellowish-gray, medium-grained sandstone with angular to subangular grains. Representative mechanical properties of both the sandstones tested are shown on Table 3.2.1.

Table 3.2.1 Representative Mechanical Properties

Rock	Young's Modulus PSI	Poisson's Ratio	Co. PSI	To PSI	γ PSI	Porosity %
Weber SS	1.5×10^6	0.3	4380	242	-	-
Ditch Creek SS	0.96×10^6	0.3	5430	523	134	16.8

3.3 Equipment and Procedures

The equipment used in carrying out the experimental program consisted of a modified, Bureau of Reclamation type triaxial cell, a Soil Test volume change indicator, a Tinius-Olsen 400,000 pound capacity testing machine, a Sanborn six-channel recorder, and miscellaneous other laboratory equipment. A schematic diagram of the test set-up is shown on Fig. 3.3.1. Tests were run on dry samples

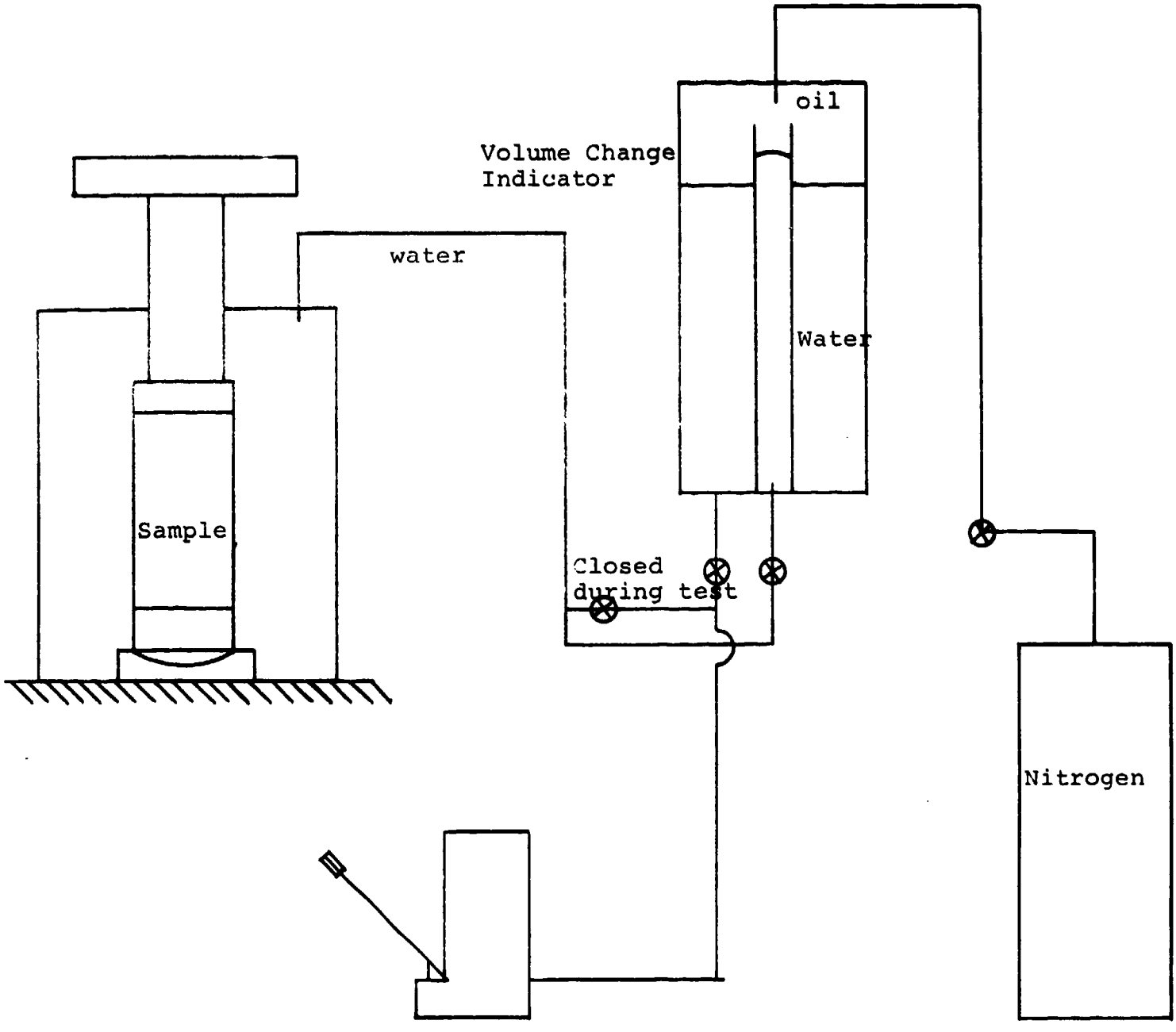

Fig. 3.3.1 Test set up

at confining pressures ranging from approximately 100 psi to 400 psi.

Confining pressures were held essentially constant during each test by applying the pressure through a large (75,000 cc) chamber containing nitrogen. Since the maximum volume change recorded was of the order of 5 cc, confining pressures were held constant to within 0.007%. No change in confining pressure could be detected with the pressure gages used. Confining pressure magnitudes were limited by the pressure capacity of the Soil Test volume change indicator which consisted of a plexiglass cylinder containing a graduated tube. A blue dye was added to the confining fluid to facilitate reading volume changes.

Samples tested were approximately 2 in. diameter with length to diameter ratios from 2 to 2.5. Sample ends were finished with a surface grinder to insure that ends were smooth and parallel to within .001 inches.

Six strain gages of 1/4 inch grid length were placed on each sample. Strain gage lead wires were brought out of the triaxial chamber through a hole in the ram. Strains were recorded on the Sanborn 6-channel recorder or by hand using standard laboratory strain gage equipment.

One sample was prepared with 40 strain gages (20 vertical and 20 horizontal) in 2-gage pairs. Strain gage lead wires were taken from the triaxial cell through a specially fabricated hollow piston. Since we desired to read all 40 gages essentially simultaneously, a multiplexing unit

was required to multiplex the data onto magnetic tape. No commercial multiplexing unit was available to us. Furthermore, no funds were available for the purchase of a multiplexer. Therefore, an attempt was made to fabricate a switching bridge type multiplexer. This attempt failed primarily due to the magnitude of transients involved in the switching. In the spring of 1976, a multiplexer was assembled using MOS chips and another attempt was made to collect the data. Unfortunately, the common lead for all the strain gages shorted out just as the test was started. The test has been delayed until the shorted lead can be repaired and the tape recorder again becomes available.

3.4 Discussion of Results

Typical results from the triaxial tests on four samples of Weber Sandstone are shown on Figures 3.4.1 through 3.4.5. For each sample the dilatometer (volume change indicator) readings versus vertical strain are compared with $2V_o\varepsilon_t$ versus vertical strain where V_o is the original volume of the sample and ε_t is the tangential strain measured by electrical resistance strain gages. Vertical stress versus vertical strain points are plotted on the same figures for reference.

Neglecting the deformation of the apparatus and assuming that the sample deforms as a right circular cylinder, the dilatometer data should coincide with the $2V_o\varepsilon_t$ data. This may be seen as follows. After deformation, the radius

$$r = r_o(1+\varepsilon_r) \qquad (3.4.1)$$

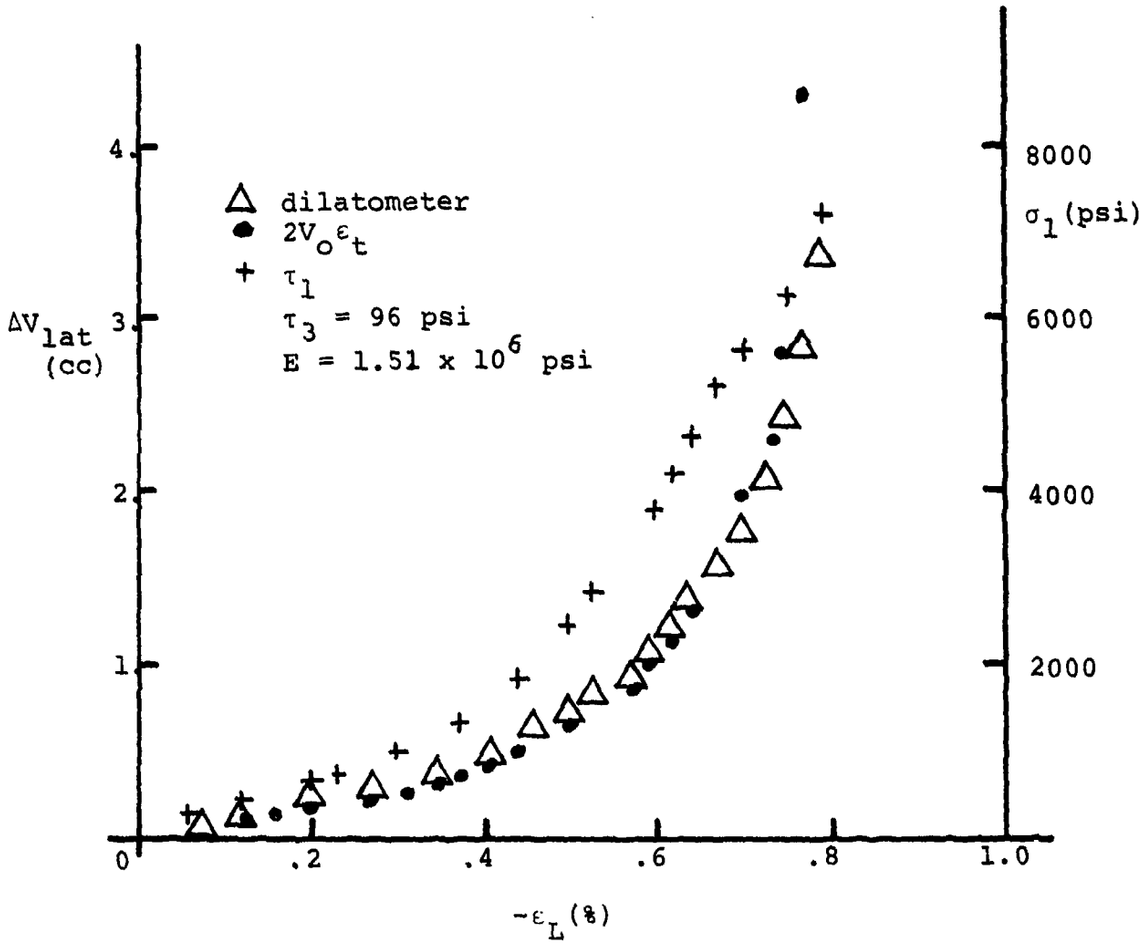

Fig. 3.4.1 Experimental results for Weber SS sample G3

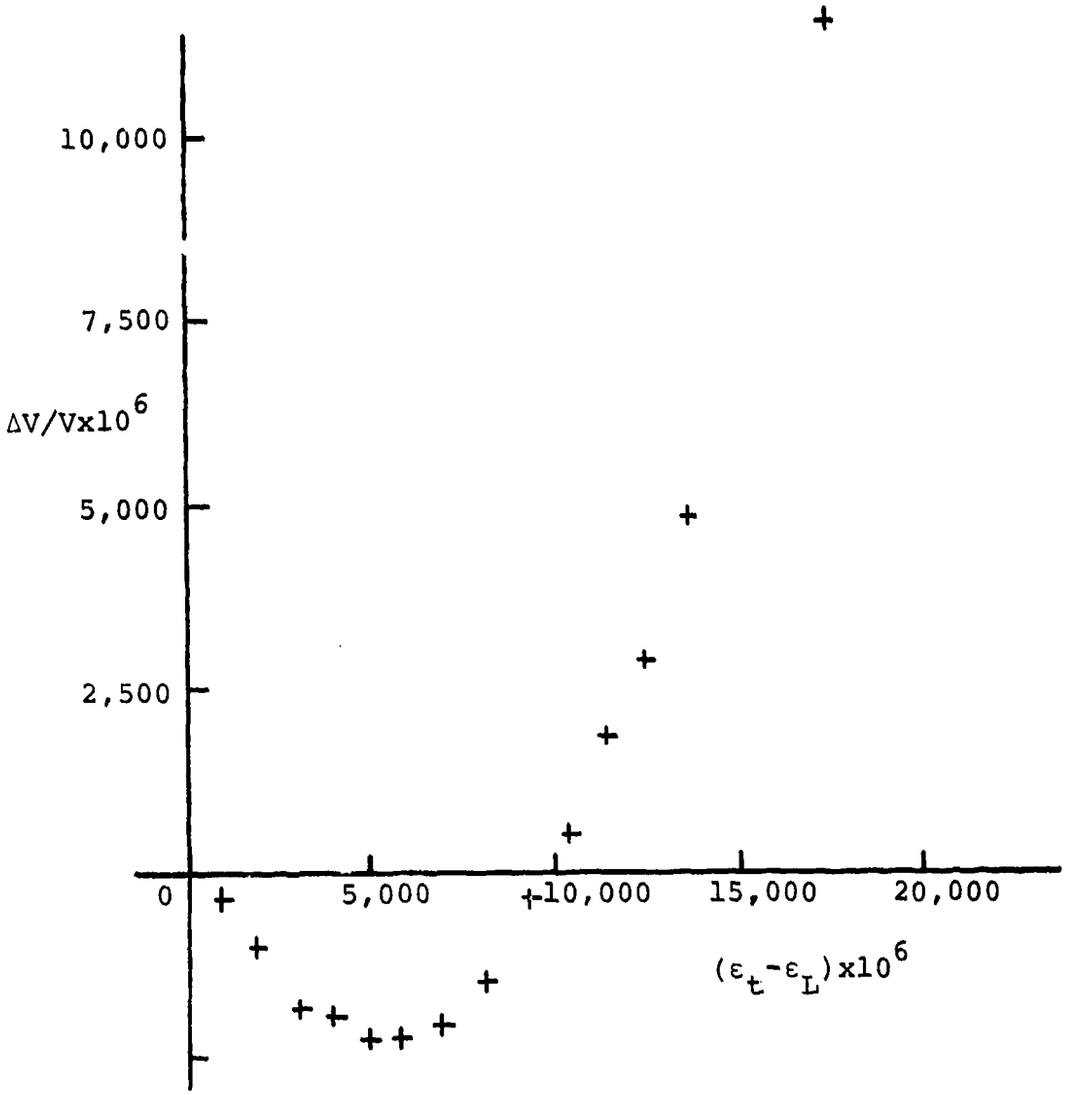

Fig. 3.4.2 Experimental results for Weber SS sample G3 (cont.)

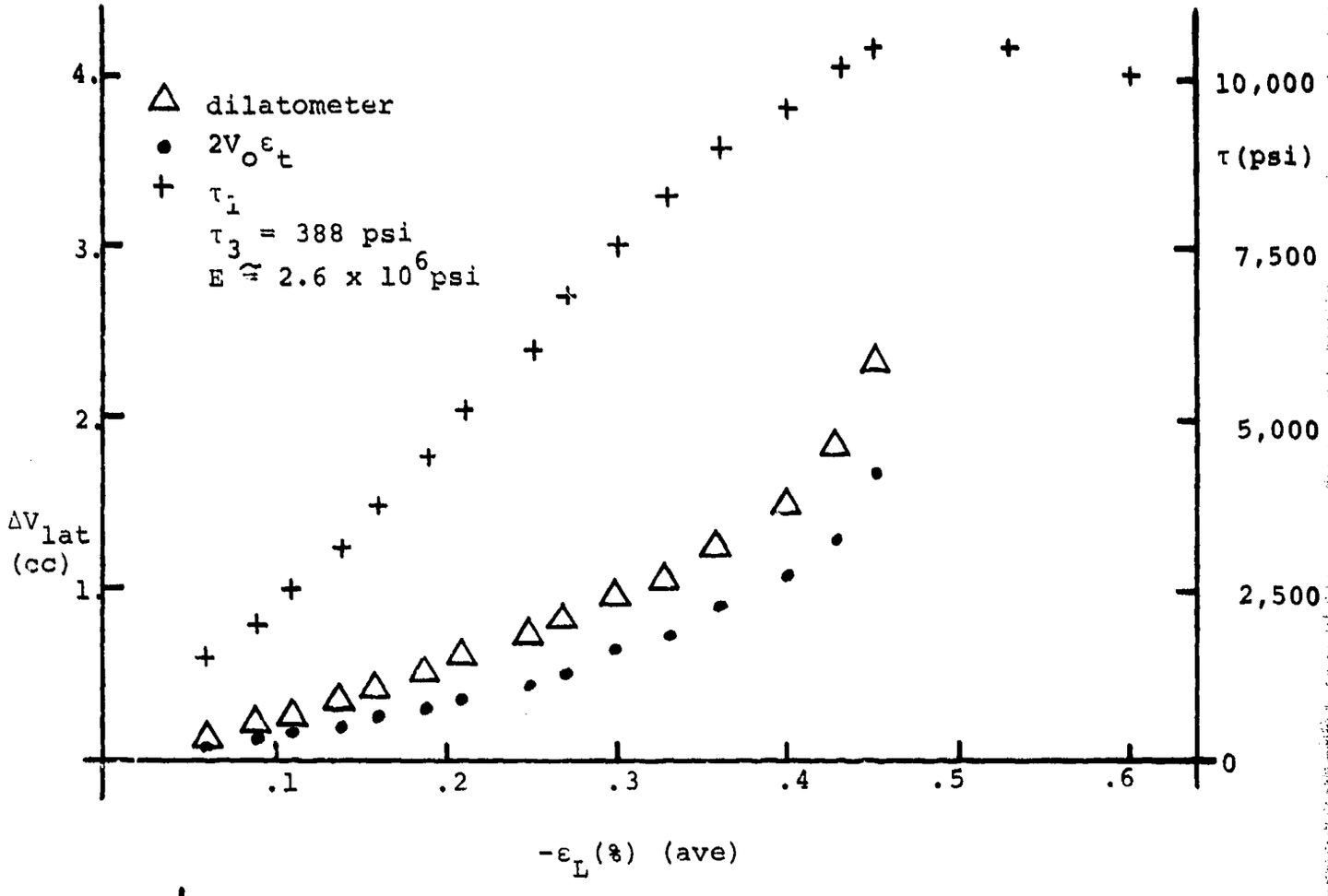

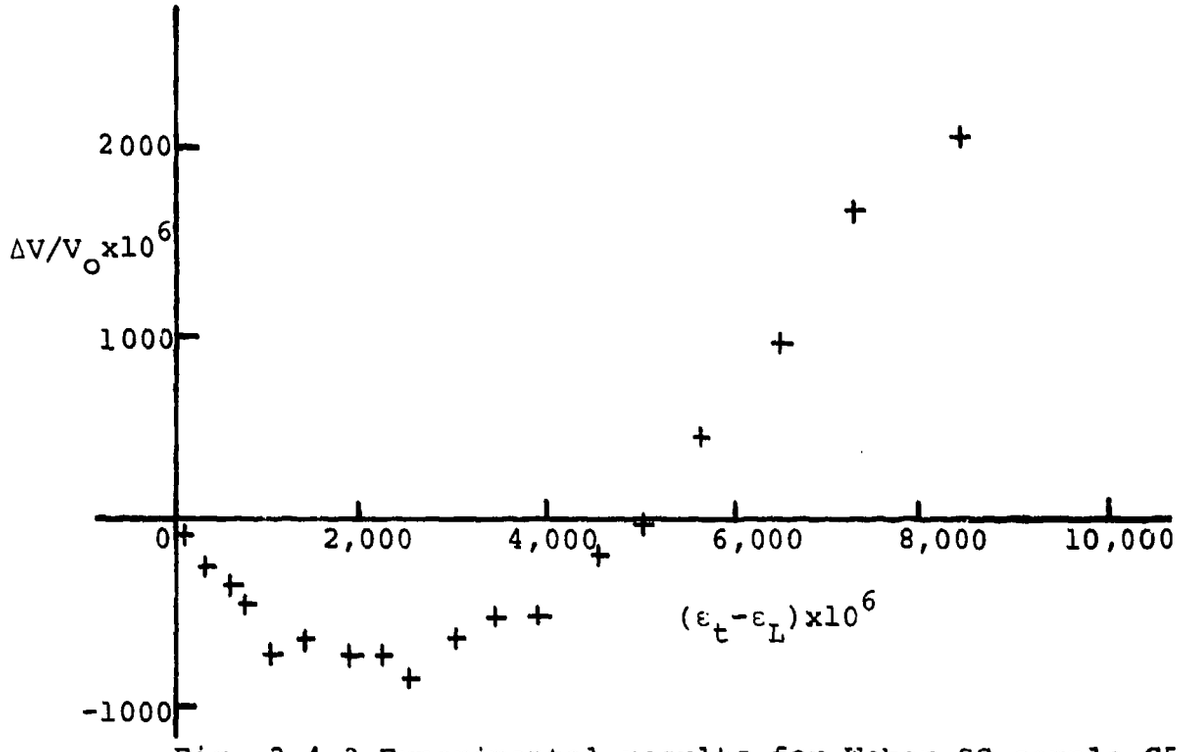

Fig. 3.4.3 Experimental results for Weber SS sample G5

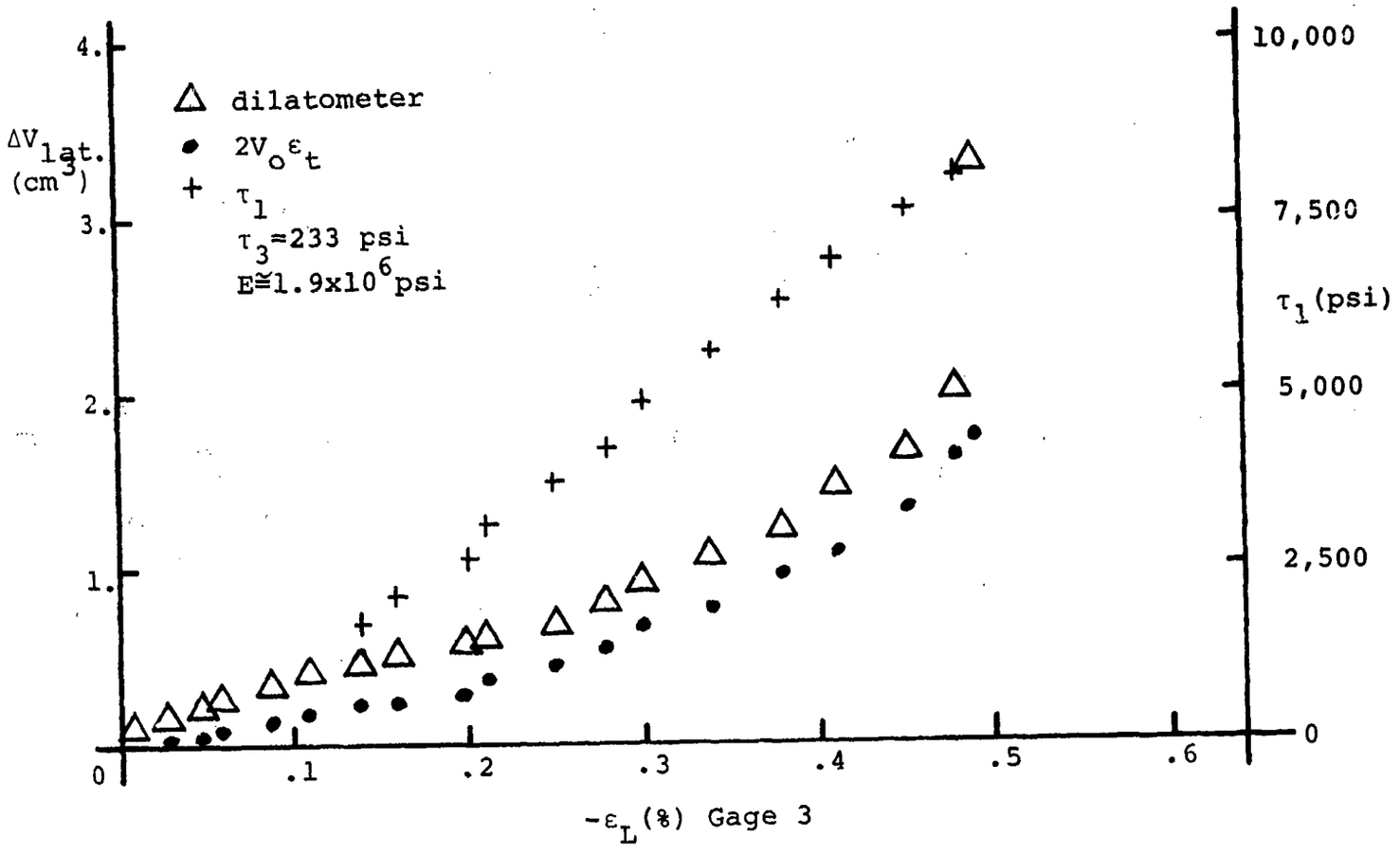

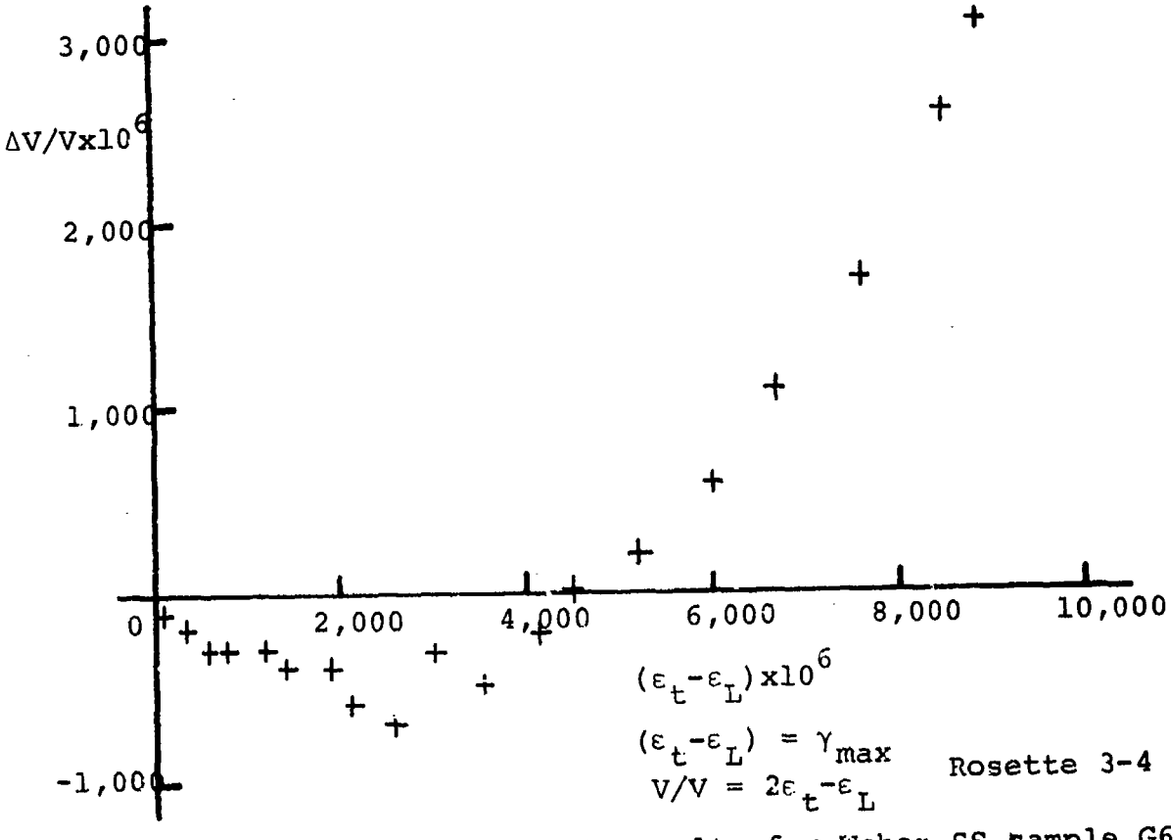

Fig. 3.4.4 Experimental results for Weber SS sample G6

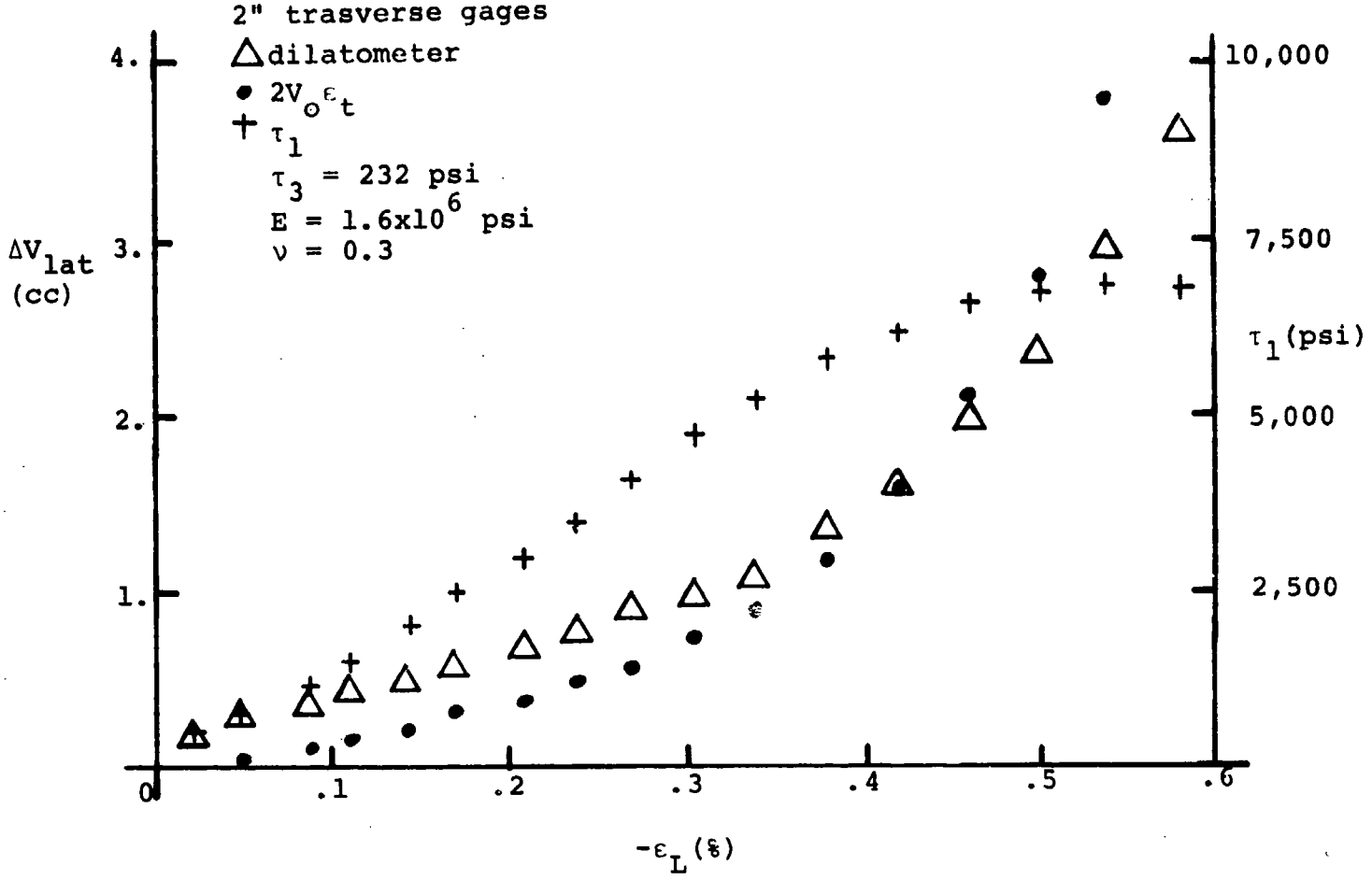

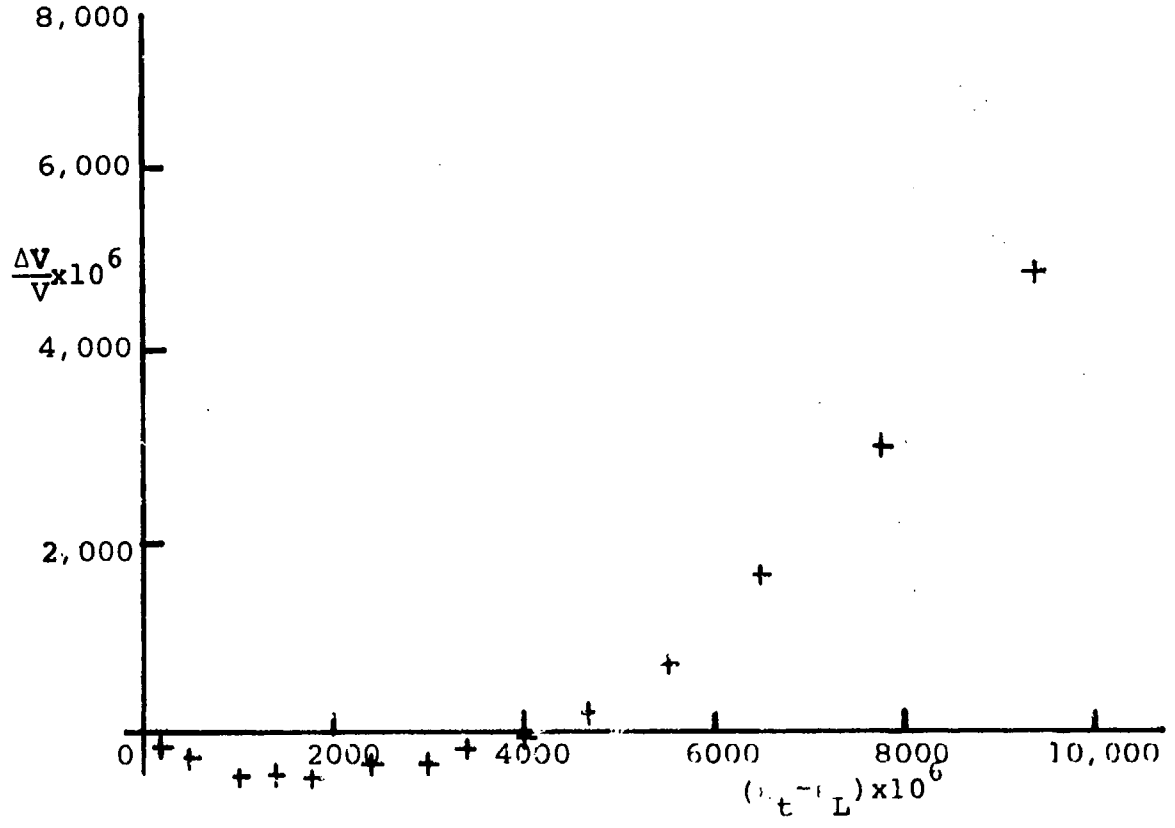

Fig. 3.4.5 Experimental results for Weber SS sample G7

where r_o is the original radius. Similarly the length after deformation is

$$L = L_o(1+\varepsilon_v) \tag{3.4.2}$$

where L_o is the original length. Neglecting second order terms, the cross-sectional area, A, becomes

$$A = \pi r_o^2(1+2\varepsilon_r) = A_o(1+2\varepsilon_r) \tag{3.4.3}$$

Neglecting the deformation of the stiffer steel ram and hemispherical seat in the triaxial cell, the hydraulic volume change indicator (dilatometer) should read a change in volume, ΔV_{lat}, equal to the annular area increase of the sample times the length. Thus,

$$\Delta V_{lat} = (A-A_o)L=\{A_o(1+2\varepsilon_r)-A_o\}L_o)1+\varepsilon_v) \tag{3.4.4}$$

which after neglecting second order effects becomes

$$\Delta V_{lat} = 2\varepsilon_r A_o L_o = 2V_o\varepsilon_r = 2V_o\varepsilon_t \tag{3.4.5}$$

since $V_o = A_o L_o$ and $\varepsilon_r=\varepsilon_t$ for a sample deforming as a right circular cylinder.

Experimental results indicate good agreement between the dilatometer readings and $2V_o\varepsilon_t$. Value of $2V_o\varepsilon_t$ typically fall below the dilatometer readings particularly for lower values of axial strain. This discrepancy is probably due to the fact that the dilatometer measures the total increase in lateral volume including that of the ram and the hemispherical seat while these effects are neglected in calculating the ΔV_{lat} from $2V_o\varepsilon_t$. With a sufficient number of tests, it may be possible to calibrate the apparatus to account for the additional change in volume registered on the volume change indicator and thus improve

the agreement between the two methods. No attempt was made in this study to calibrate the dilatometer for this effect.

An expression for the change in volume divided by the original volume ($\Delta V/V$) may be derived as follows. From Eqs. (3.4.2) and (3.4.3), the volume after deformation is

$$V = AL = \{A_o(1+2\varepsilon_r)L_o\}(1+\varepsilon_v) \tag{3.4.6}$$

After neglecting second order effects and noting that $V_o = A_o L_o$, we have

$$V = V_o(1+\varepsilon_v+2\varepsilon_r) \tag{3.4.7}$$

Then the change in volume becomes

$$\Delta V = V-V_o = V_o(\varepsilon_v+2\varepsilon_r) \tag{3.4.8}$$

and

$$\Delta V/V_o = \varepsilon_v+2\varepsilon_r = \varepsilon_v+2\varepsilon_t \tag{3.4.9}$$

where $\varepsilon_t=\varepsilon_r$ for axially symmetric deformation. The right hand side of Eq. (3.4.9) represents the trace (first invarient) of the linear strain tensor for axially symmetric deformation and is a familiar result from continuum mechanics. This derivation is presented here to emphasize that $\Delta V/V_o$ depends only on changes in geometry and is independent of any material model.

Using Eq. (3.4.9), we can calculate $\Delta V/V_o$ for each two-gage rosette consisting of one vertical and one tangential strain gage. Experimental results are presented for each sample by plotting $\Delta V/V_o$ versus the maximum shearing strain $\gamma_{max} = \varepsilon_t-\varepsilon_v$. Each of these curves exhibits an initial negative slope which then flattens out and finally increases

rapidly as failure is approached indicating dilation and emphasizing the relationship between volumetric deformation and shear deformation in the post elastic range. Each of these curves has the same general shape that has been observed by many soil mechanics investigators during triaxial tests on dense sands.

It should be noted that as long as the sample remains linearly elastic, the $\Delta V/V_o$ should decrease as γ_{max} increases since in this case

$$\varepsilon_t = -\nu\varepsilon_v \tag{3.4.10}$$

Then

$$\Delta V/V_o = \varepsilon_v(1-2\nu) \tag{3.4.11}$$

and

$$\gamma_{max} = \varepsilon_t - \varepsilon_v = -\varepsilon_v(1+\nu) \tag{3.4.12}$$

The slope of the curve in the elastic range should then be

$$\text{Slope} = -(1-2\nu)/(1+\nu) \tag{3.4.13}$$

For Poisson's ratio $\nu = 0.25$, the slope in the elastic region should be -0.4. As the inelastic region is approached the apparent Poisson's ratio tends to increase and the Slope approaches zero as ν approaches 0.5. The Slope becomes positive as the negative ratio of tangential to vertical strain exceeds 0.5. Conservation of mass precludes this ratio from exceeding 0.5 for a continuous material. Thus, we conclude that microcracks must be opening in the sample. These microcracks could account for the relatively high tangential strains and the corresponding dilation of the sample.

It is interesting to compare the experimental $\Delta V/V_o$ versus γ_{max} curves with the curve assumed by Frank (1965). Since Frank neglected elastic deformation, his curve would start at the point where the slope of our experimental curve is zero and the sample is beginning to dilate. The curves agree then in shape although the experimental curves do not indicate the change in curvature assumed by Frank. This may be due to the fact that the strain gages used are not capable of measuring large strains and suggests that another technique should be developed to measure large deformations particularly in the failure zone.

4. CONCLUSIONS

The objectives of this study include a theoretical study of the nature of mechanical instabilities, a numerical study to illustrate the behavior predicted by the theoretical study, and a laboratory study of basic dilatational response of one sandstone under triaxial test conditions. Mechanical instability is defined as a non-trivial increase in kinetic energy resulting when an equilibrium state is perturbed by an energy input of negligible magnitude.

From the theoretical study, we conclude that an equilibrium state of other than minimum total potential energy can exist in the presence of a sufficient dissipative mechanism. However, the presence of a dissipative mechanism does not insure the stability of an inherently unstable system. The importance of the rate of energy dissipation is emphasized by Eq. (1.3.9). Further importance is given to the rates of energy input and dissipation in the numerical study where if fluid is pumped into the system at a slow enough rate compared to the dissipative characteristics of the system, the fluid head simply decays after pumping stops and the blocks remain stable.

The numerical model also illustrates the coupling between the spring-mass part of the system and the fluid flow system. This one-dimensional model allows numerical fluid injection experiments to be run. By varying parameters in the model, both wave propagation and diffusion

results can be obtained in the fluid while the block masses may remain fixed or show either creep or earthquake events.

Relative to the control of earthquakes, this study suggests that potential energy be reduced by controlled smaller earthquakes and creep events. Furthermore, the rate of external work done on a fault zone by fluid injection may provide a means of controlling the size of the induced event. The model also suggests that earthquake control might be accomplished by increasing the capacity for energy dissipation in the fault zone. This may be possible by injecting a special fluid at a very low rate. This fluid would have to be miscibile with the pore fluid and have a viscosity that increases with time and/or temperature.

From the results of the laboratory study we conclude that the samples of Weber Sandstone do dilate under triaxial conditions with confining pressures in the 100 to 400 psi range. The shape of the dilatancy curves is similar to that reported for dense sands. Dilatancy of laboratory samples can be measured either hydraulically or by using electrical resistance strain gages. However, both techniques assume that the sample deforms as a right circular cylinder. An attempt has been made to study the spatial distribution of dilatancy by placing 40 strain gages on a single sample. Initial attempts have failed due to lack of appropriate equipment. This work is continuing on an unsponsored basis and results will be reported when they are obtained. More work is recommended on the spatial distribution of dilatancy.

5. REFERENCES

Aggarwal, Y. P., L. R. Sykes, J. Armbruster, and M. L. Sbar, Premonitory changes in seismic velocities and prediction of earthquakes, Nature, 241, 101-104, 1973.

Brace, W. F., B. W. Paulding, Jr., and C. Scholz, Dilatancy in the fracture of crystalline rocks, J. Geophys. Res. 71, 3939-3953, 1965.

Bridgman, P. W., Volume changes in the plastic stages of simple compression, J. Appl. Phys., 20, 1241-1251, 1949.

Burridge, R. and L. Knopoff, Model and theoretical seismicity, Bull. Seism. Soc. Am., 57-3, 341-371, 1967.

Crouch, S. L., Experimental determination of volumetric strains in failed rock, Int. J. Rock Mech. Min. Sci., 7, 589-603, 1970.

Denbigh, K., The principles of chemical equilibrium, Cambridge University Press, 1968.

Dieterich, J. H., Time-dependent friction in rocks, J. Geophys. Res., 77, 3690-3697, 1972.

Dieterich, J. H., Time-dependent friction as a possible mechanism for aftershocks, J. Geophys. Res., 77, 3771-3781, 1972.

Drucker, D. C. and W. Prager, Soil mechanics and plastic analysis or limit design, Quart. Appl. Math., 10, 157-165, 1952.

Edmond, J. M. and M. S. Paterson, Volume changes during the deformation of rocks at high pressures, Int. J. Rock Mechanics Min. Sci., 9, 161-182, 1972.

Finn, W. D. L., N. H. Wade, and K. L. Lee, Volume changes in triaxial and plane strain tests, J. Soil Mech. and Found. Div., ASCE, 93, 1967.

Frank, F. C., On dilatancy in relati on to seismic sources, Rev. Geophys., 3, 485-410, 1965.

Frank, F. C., A further note on dilatancy in relation to seismic sources, Rev. Geophys., 4, 405-408, 1966.

Goodman, R. E. and J. Dubois, Duplication of dilatancy in analysis of jointed rocks, J. Soil Mech. Found. Div. ASCE, 98, 399-422, 1972.

Hansen, W. R. and M. G. Bonilla, Geology of the Minila Quadrangle, Utah-Wyoming, Miscellaneous Geologic Investigations, Map I-156, U.S.G.S., Washington, D. C. 1956.

Ko, H. Y. and R. F. Scott, Deformation of sand in shear, J. Soil Mech. Found. Div., ASCE, 93, 283-311, 1967.

Ko, H. Y. and R. F. Scott, Deformation of sand at failure, J. Soil Mech. Found. Div., ASCE, 94, 883-898, 1968.

Lee, K. L. and H. B. Seed, Drained strength characteristics of sands, J. Soil Mech. Found. Div., ASCE, 93, 117-141, 1967.

Malvern, L. E., Introduction to the mechanics of a continuous medium, Prentice-Hall, Inc., 1969.

Murrell, S. A. F. and P. J. Digby, The thermodynamics of brittle fracture initiation under triaxial stress conditions, Int. J. Frac. Mech., 8, 167-173, 1972.

Nur, A., Dilatancy, pore fluids, and premonitory variations of t_s/t_p, Bull. Seismol. Soc. Amer., 62, 1217-1222, 1972.

Orowan, E., Dilatancy and the seismic focal mechanism, Rev. Geophys, 4, 395-404, 1966.

Raleigh, C. B., and M. S. Paterson, Experimental deformation of serpentinite and its tectonic implications, J. Geophy. Res., 70, 3965-3985, 1965.

Reynolds, O., On the dilatancy of media composed of rigid particles in contact, Phil. Mag., 20, 469-481, 1885.

Rowe, P. W., The stress-dilatancy relation for static equilibrium of an assembly of particles in contact, Proc. Roy. Soc., London, 269, 1962.

Rowe P. W., Stress-dilatancy, earth pressures, and slopes, J. Soil Mech. Found. Div., ASCE, 89, 37-61, 1963.

Scholz, C. H., L. R. Sykes, and Y. P. Aggarwal, Earthquake Prediction: a physical basis, Science, 181, 803-810, 1973.

Vesic, A. S. and G. W. Clough, Behavior of granular materials under high stresses, J. Soil Mech. Found. Div., ASCE, 94, 661-688, 1968.

APPENDIX I: CONSERVATION OF MECHANICAL ENERGY

Eq. (1.3.1) is a statement of the conservation of mechanical energy and may be derived from the first integral of the equation of motion. The equation of motion may be written for a mass as

$$\sum_k F_i^k = M\frac{dv_i}{dt} \tag{A.1}$$

where F_i^k is a component of force k in the direction of "i" while M is the mass, v_i is the component of velocity in the direction "i" and t is time. The summation is over all forces acting on the mass. If we now multiply Eq. (A.1) by $v_i dt$ and integrate from point 1 to 2, we have

$$\sum_k \int_1^2 F_i^k v_i dt = \int_1^2 M\frac{dv_i}{dt} v_i dt \tag{A.2}$$

where summation from i=1 to 3 is indicated by the repeated subscript. Noting that $v_i = dX_i/dt$ where X_i is the displacement component in direction "i," Eq. (A.2) may be written as

$$\sum_k \int_1^2 F_i^k dX_i = \int_1^2 d(\tfrac{1}{2}mv^2) = \int_1^2 d(KE) \tag{A.3}$$

By definition, the work done by F^k in going from point 1 to point 2 is

$$_1W_2^k = \int_1^2 F_i^k dX_i \tag{A.4}$$

Then Eq. (A.3) becomes

$$\sum_k {}_1W_2^k = (KE)_2 - (KE)_1 = \Delta KE \tag{A.5}$$

If a gravitational field is present, one value of k represents the work done by gravity in going from point 1 to point 2. By definition,

$$_1W_2^{grav} = -(PE_2 - PE_1) = -\Delta PE \tag{A.6}$$

Then Eq. (A.5) becomes

$$\sum_K {}_1W_2^k = \Delta KE+\Delta PE \tag{A.7}$$

where the left side now excludes the work done by gravity.

If we now write,

$$\sum_K {}_1W_2^k = {}_1W_2 + {}_1W_2^f \tag{A.8}$$

Eq. (A.7) becomes

$$\Delta KE+\Delta PE = {}_1W_2+{}_1W_2^f \tag{A.9}$$

which is exactly Eq. (1.3.1).